

This is the accepted manuscript made available via CHORUS. The article has been published as:

Radiation burst from a single γ -photon field

R. N. Shakhmurov, F. Vagizov, and O. Kocharovskaya

Phys. Rev. A **84**, 043820 — Published 11 October 2011

DOI: [10.1103/PhysRevA.84.043820](https://doi.org/10.1103/PhysRevA.84.043820)

Radiation burst from a single gamma-photon field

R. N. Shakhmurov,^{1,2} F. Vagizov,^{3,2} and O. Kocharovskaya²

¹*Kazan Physical-Technical Institute, Russian Academy of Sciences,*

10/7 Sibirsky Trakt, Kazan 420029 Russia

²*Department of Physics and Institute for Quantum Studies,*

TAMU, College Station, Texas 77843-4242, USA

³*Kazan Federal University, 18 Kremlyovskaya St. Kazan 420008 Russia*

Abstract

The radiation burst from a single gamma-photon field interacting with a dense resonant absorber is studied theoretically and experimentally. This effect was discovered for the first time by P. Helisto *et al.*, Phys. Rev. Lett. **66**, 2037 (1991) and it was named "gamma echo". The echo is generated by 180-degree phase shift of the incident radiation field, attained by an abrupt change of the position of the absorber with respect to the radiation source during the coherence time of the photon wave packet. Three distinguishing cases of "gamma echo" are considered, i.e., the photon is in exact resonance with the absorber, close to resonance (on the slope of the absorption line), and far from resonance (on the far wings of the resonance line). In resonance the amplitude of the radiation burst is two times larger than the amplitude of the input radiation field just before its phase shift. This burst was explained by P. Helisto *et al.* as a result of constructive interference of the coherently scattered field with the phase shifted input field, both having almost the same amplitude. We found that out of resonance the scattered radiation field acquires an additional component with almost the same amplitude as the amplitude of the incident radiation field. The phase of the additional field depends on the optical thickness of the absorber and resonant detuning. Far from resonance this field interferes destructively with the phase-shifted incident radiation field and radiation quenching is observed. Close to resonance three fields interfere constructively and the amplitude of the radiation burst is three times larger than the amplitude of the input radiation field.

PACS numbers: 42.50.Gy

I. INTRODUCTION

Quantum information technology requires the development of methods of the operation with single photons, i.e., storage and retrieval, photon shaping, etc. Since single photons are suggested to carry quantum information between nodes in a quantum network, two kind of nodes were proposed. One is based on a quantum electrodynamics scheme using a strong coupling of a single atom with a single cavity mode (see, for example, Ref. [1]). The other is based on the interaction of a single photon with ensemble of atoms (see, for example, Refs. [2–6]). Ensemble approach has an advantage of large number of particles interacting with the radiation field, which results in a collective enhancement of the atom-field interaction.

Collective scattering of a single photon by an ensemble of N particles is a coherent process since all quantum paths of the photon interfere. Therefore, the probability amplitude of the scattered radiation field is nonlinearly dependent on N , see Refs. [7, 8], while the probability amplitude of the incoherent scattering in 4π angle is proportional only to N .

In the Feynman lectures [9] one can find an interesting explanation of the phenomena of absorption and dispersion of light by a linear medium. According to Feynman the light, transmitted by any sample, can be considered as a result of the interference of the input wave, as if it would propagate in vacuum, with the secondary wave radiated by the linear polarization induced in the medium. In an optically thick sample these two waves are obviously of the same amplitude and 180° out of phase, which leads to a fully destructive interference.

In Refs. [10, 11] it was proposed and experimentally implemented to bring the secondary wave in phase with the incident radiation by abrupt change of its phase. A single-photon radiation field is considered as a wave packet. The source starts to emit this wave packet at a particular time t_0 . If the photon source is moved abruptly at a time $t_1 > t_0$, changing almost instantaneously its position with respect to the absorber, the phase of the single photon wave packet, φ_s , also changes at t_1 . If $\varphi_s = \pi$, the incident radiation becomes in phase with the scattered radiation and they interfere constructively. This interference is seen as a radiation burst whose amplitude is doubled (in some cases it is slightly more than doubled) and its intensity is four times larger than the intensity of the incoming radiation field.

The experiments, reported in Refs. [10, 11], are performed with the absorber, which is in exact resonance with the source. In this paper we study nonresonant excitation and show

that for a particular detuning from resonance three fields interfere constructively, i.e., the incoming field just after its phase shift, a transient scattered field, induced at an earlier time by the leading edge of the photon wave packet, and a field, formed in the absorber before the phase shift and propagating with a slow group velocity. The phase of the third field depends on optical thickness of the absorber and resonant detuning. Maximum amplitude of the radiation burst is nearly 3 times larger than the amplitude of the incident radiation just before the phase shift and its intensity is 9 times larger (in some cases 10 times larger). Such a revival of a single photon radiation field can be applied for photon storage and retrieval or/and photon shaping, which are in a scope of quantum computing and quantum information. A kind of photon storage and photon shaping was studied using synchrotron radiation (see, for example, Refs. [12–14])

The paper is organized as follows. In Sec. II we represent the general formalism of the description of multiple scattering of a photon in an absorber with a single resonance. In Sec. III we consider an instantaneous phase shift of a single photon radiation field and transients induced in a thick absorber. In Sec. IV we consider an instantaneous frequency shift of the radiation field. In Secs. V and VI experimental results and their discussion are represented.

II. PHOTON FILTERING THROUGH A RESONANT ABSORBER

In this section we present generalities of the time-domain Mössbauer spectroscopy using the time delayed coincidence measurements (TDCM) of two photons, emitted in a cascade by an excited state particle. In TDCM the detection of the first photon in the cascade heralds the emission of the second photon, which is applied for spectroscopy of an absorber, containing resonant nuclei.

The most popular Mössbauer isotope, ^{57}Fe , incorporated into a solid, is usually used as an absorber. The appropriate gamma-photon source for ^{57}Fe consists of a macroscopically large number of ^{57}Co nuclei, incorporated into another solid to have an appreciable fraction of emitted radiation without recoil. ^{57}Co decays by electron capture to ^{57m}Fe , which decays in turn by emission of a 122 keV photon, followed by a 14.4 keV photon (competing with internal conversion) to the ground state. If the number of ^{57}Co nuclei in the source is small enough, i.e., the activity of the source is small, the long half-life of ^{57}Co (271.8 days) secures that during the life-time of 14.4 keV state (141 ns), almost no decay event of another ^{57}Co

in the absorber takes place.

Quantum mechanical calculation of the conditional probability amplitude $a(t)$ of the second photon, if the detection of the first photon in the cascade at time t_0 took place, gives (see, Ref. [15])

$$a(t) = \Theta(t - t_0) e^{-(i\omega_s + \gamma)(t - t_0)}, \quad (1)$$

where ω_s is the frequency of the 14.4 keV photon, 2γ is the decay rate of the 14.4 keV state (radiative and nonradiative if present), and $\Theta(t)$ is the Heaviside step function. Eq. (1) is similar to the definition of the radiation field for the source photon, introduced in Ref. [7] within a classical theory of gamma-photon propagation in a dense resonant medium. Here the maximum of the probability amplitude $a(t)$ is normalized to unity and the distances from the source to the detector 1 (d_1) and to the detector 2 (d_2) are neglected since d_1/c and d_2/c are much smaller than the lifetime of the 14.4 keV state, where c is the speed of light in vacuum.

The probability amplitude of the second photon wave packet has a sharply rising leading edge at $t = t_0$ and an exponentially decaying tail. The former is defined by the time t_0 at which the source is formed in the 14.4 keV state and the latter specifies the coherence time of the photon $\tau_{\text{ph}} = 1/\gamma$. Such a time dependence of the single-photon field has been detected, using radiation of a single nucleus in time delayed coincidence measurements of gamma photons emitted in a nuclear cascade [7, 16–20]. Usually ^{57}Co nuclei are incorporated into a solid, which does not produce quadrupole and Zeeman magnetic splitting of nuclear spin states. In such a case the source emits a single frequency radiation field (14.4 keV).

In TDCM technique a macroscopic absorber is placed in between the source and the detector for the second photon. For simplicity we limit our consideration to an absorber with a single absorption line. We consider the case when nuclei are randomly distributed in the host. Hence, no Bragg scattering is present. Then, an incident photon, represented by a plane wave at the input of the absorber, is scattered coherently only in the forward direction by all nuclei, and propagates inside (see, for example, Ref. [21]). There is no coherent scattering in other directions because of random phase. Incoherent scattering in other directions may take place but its probability is much smaller than the probability of coherent scattering in the forward direction.

In the classical theory [7], according to standard methods in electrodynamics, the amplitude of the radiation field at the output of the resonant absorber of physical thickness l

is

$$a(l, t - t_0) = \frac{1}{2\pi} \int_{-\infty}^{+\infty} A_0(\nu) e^{-i(\omega_s + \nu)(t - t_0) - \alpha(\nu)l} d\nu, \quad (2)$$

where l/c is neglected, $A_0(\nu)$ is the Fourier transform of the amplitude $a_0(t) = a(t) \exp[i\omega_s(t - t_0)]$ of the input radiation, which is

$$A_0(\nu) = \frac{i}{\nu + i\gamma}, \quad (3)$$

and $\alpha(\nu)$ is the transmission function. Eq. (2) is similar to the expression for the spatial wave function of the single-photon radiation field at the output of a thick absorber, which is derived within a quantum mechanical theory by Harris in Ref. [8] [see Eq. (40) in this reference].

Here we adopt the Fourier transform of the form

$$F(\nu) = \int_{-\infty}^{+\infty} f(t) e^{i\nu(t - t_0)} dt. \quad (4)$$

For the absorber with a single resonance line, $\alpha(\nu)$ is

$$\alpha(\nu) = \frac{i\gamma\alpha_B/2}{\nu + \Delta + i\gamma}, \quad (5)$$

where $\Delta = \omega_s - \omega_a$ is the detuning of ω_s from the resonant frequency, ω_a , of the absorber and α_B is the Beer's law absorption coefficient applicable to a monochromatic radiation tuned in resonance. With this coefficient the conventional definition of the optical thickness of the absorber for a resonant excitation, is $T = \alpha_B l$. The quantum mechanical definition of T is $T = nl\sigma_0 f_a$, where n is the density of ^{57}Fe nuclei in the absorber, σ_0 is the cross section of resonant absorption for the 14.4 keV transition, and f_a is the recoilless fraction of the gamma-ray absorption in the absorber.

For a single photon radiation field (1), the integral in Eq. (2) has been calculated in Ref. [7] with the help of the generating function for the Bessel function. If the nuclei in the absorber have a single absorption line tuned in exact resonance with the source photon ($\Delta = 0$), then the amplitude of the output radiation is

$$a(l, t) = \Theta(t) e^{-i\omega_s t - \gamma t} J_0\left(2\sqrt{bt}\right), \quad (6)$$

where $J_0(x)$ is the zero-order Bessel function, $b = T\gamma/2$, and $t_0 = 0$.

If $b \gg \gamma$ the decay of the radiation field at the output of a thick absorber is not more defined by the function $\exp[-\gamma(t - t_0)]$, but it is ruled by the Bessel function

$J_0[2\sqrt{b(t-t_0)}]$, whose decay rate is $\sim b$ at the initial stage (after t_0 and before the first zero of $J_0[2\sqrt{b(t-t_0)}]$).

As it is explained, for example, in Ref. [10], the accelerated decay of the radiation field at the output of a thick absorber is due to destructive interference of the incident radiation with coherently forward-scattered radiation field, i.e. this is a dynamical process, which is reversible in principle. Therefore, just a π phase-shift of the input radiation field at a later time changes destructive interference to constructive interference of the input radiation field with the scattered field coming from the absorber excited at an earlier time. This change results in a revival of the radiation field seen as a radiation burst.

For the nonresonant case, when the frequency of the source ω_s is detuned from the center of the absorption line of nuclei in the absorber, the result of the calculation of the integral in Eq. (2) for the probability amplitude $a(l, t)$ of the radiation field at the output of the absorber becomes quite complicated. It is described by the infinite sum of the Bessel functions of the ascending integer order, multiplied by the complex coefficients depending on b , Δ , and t , see Ref. [7]. Actually there are two such expressions, one is for $b > \Delta$ and the other is for $b < \Delta$. Both expressions converge very slowly and one has to take into account many terms (between 50 and 100) of these sums to obtain an accurate approximation of the integral in Eq. (2).

To simplify the analysis and obtain clear asymptotic expressions we use the response function technique, applied in Ref. [10]. Then Eq. (2) is reduced to

$$a(l, t) = e^{-i\omega_s t} \int_{-\infty}^{+\infty} a_0(t - \tau) R(\tau) d\tau. \quad (7)$$

where we set $t_0 = 0$ for simplicity and

$$R(t)e^{-i\omega_s t} = \delta(t)e^{-i\omega_s t} + a_{sc}(t)e^{-i\omega_a t}, \quad (8)$$

is the output field from the resonant absorber if the input field is a short pulse, described by the delta function, $\delta(t)$. The second term in Eq. (8), which is proportional to

$$a_{sc}(t) = -a_0(t) \sqrt{\frac{b}{t}} J_1(2\sqrt{bt}), \quad (9)$$

can be considered as a scattered field, produced by a short delta-like pulse. The response function $R(t)e^{-i\omega_s t}$, Eq. (8), for the absorber with a single resonance was calculated in Refs. [22–24].

Direct integration of the integral in Eq. (7) gives

$$a(l, t) = a_0(t)e^{-i\omega_s t} [1 + f_{sc}(t)]. \quad (10)$$

where

$$f_{sc}(t) = -\int_0^t e^{i\Delta\tau} \sqrt{\frac{b}{\tau}} J_1(2\sqrt{b\tau}) d\tau. \quad (11)$$

Integrating by parts the integral in Eq. (11), we obtain

$$f_{sc}(t) = f_{sc1}(t) + f_{sc2}(t), \quad (12)$$

where

$$f_{sc1}(t) = J_0(2\sqrt{bt}) e^{i\Delta t} - 1, \quad (13)$$

$$f_{sc2}(t) = -i\Delta \int_0^t J_0(2\sqrt{b\tau}) e^{i\Delta\tau} d\tau. \quad (14)$$

With this result we express Eq. (10) for the output radiation as follows

$$a(l, t) = a(t) + a_{fs}(t) + a_{sl}(t), \quad (15)$$

where $a(t)$ is the radiation field, passed through the absorber without scattering, $a_{fs}(t) = a(t)f_{sc1}(t)$ is a part of the scattered radiation, which develops fast, and $a_{sl}(t) = a(t)f_{sc2}(t)$ is the other part of the scattered radiation, which we name the slow radiation, since it develops with slower rate than $a_{fs}(t)$ and propagates with a slow group velocity (see discussion below and in the Appendix).

In a thick absorber ($b \gg \gamma$) and for resonant detuning Δ satisfying the condition $b \gg |\Delta| \sim \gamma$, the scattered radiation $a_{fs}(t)$ develops fast. Its effective amplitude $f_{sc1}(t)$, defined without exponential factor $\exp(-\gamma t)$, is close to -1 for $bt > 1$ (i.e., $t > 1/b$). The fast-scattered radiation is in antiphase with the incoming radiation and their sum is

$$a(t) + a_{fs}(t) = a_0(t) J_0(2\sqrt{bt}) e^{-i\omega_a t}, \quad (16)$$

which oscillates with the resonant frequency of the absorber ω_a and decays with the rate $\sim b$.

In resonant case ($\omega_s = \omega_a$) the slow part of the scattered radiation is zero [$a_{sl}(t) = 0$] and the amplitude of the output radiation, $a(l, t)$, coincides with $a(t) + a_{fs}(t)$, see Eq. (6). Thus, only the fast scattered field

$$a_{fs}(t) = a(t) \left[J_0(\sqrt{\beta t}) - 1 \right] \quad (17)$$

is developed in the absorber. Its destructive interference with the incident radiation is seen as absorption.

Out of resonance ($\omega_s \neq \omega_a$) the fast scattered field is

$$a_{fs}(t) = a_0(t) \left[J_0 \left(\sqrt{\beta t} \right) e^{-i\omega_a t} - e^{-i\omega_s t} \right], \quad (18)$$

and the slow part of the scattered radiation field $a_{sl}(t)$ is not zero anymore. Its effective amplitude $f_{sc2}(t)$, defined without exponential factor $\exp(-\gamma t)$, has the asymptote

$$\lim_{t \rightarrow +\infty} f_{sc2}(t) = e^{-ib/\Delta}, \quad (19)$$

see Ref. [25]. Thus, for large t , the amplitude of the fast scattered field, $a_{fs}(t)$, tends to the value $-a(t)$, while the amplitude of the slow scattered field, $a_{sl}(t)$, tends to $a(t) \exp(-ib/\Delta)$. The total amplitude of the scattered field, $a(t)f_{sc}(t)$, has the limit $a(t)[\exp(-ib/\Delta) - 1]$. If $b/\Delta = 2\pi m$, where m is a natural number, the effective amplitude of the scattered field, $f_{sc}(t)$, is zero. If $b/\Delta = \pi(2m + 1)$ the effective amplitude of the scattered field is -2 . In both cases the absorber becomes transparent for the radiation field since its interference with the scattered field does not change the amplitude of the radiation field, but its phase, i.e., $a(t) + a_{sc}(t) = \pm a(t)$. For arbitrary value of b/Δ we have $a(t) + a_{sc}(t) = a(t) \exp(-ib/\Delta)$.

The transparency of the absorber is explained in the Appendix, where the rate of the development of slow light is also evaluated. Here we briefly outline two important points of the formation of slow light. If $|\omega_s - \omega_a| \sim \gamma$, the central components of the photon spectrum, close to ω_s , play a crucial role. These components experience less absorption because of the reduced value of $\text{Re}[\alpha(\nu)]$ in the transmission integral, Eq. (2). Moreover, due to the normal dispersion, defined by $\text{Im}[\alpha(\nu)]$, they propagate with a small group velocity (smaller than c), see Refs. [26–31].

III. INSTANTANEOUS PHASE SHIFT OF THE INCIDENT RADIATION FIELD

In this section we consider the influence of an instantaneous π -shift of the phase of the incident field $a(t)$ on the output radiation field from a thick absorber. This phase shift can be realized by the sudden change of the distance between the source and the absorber, for example, by a shift of the source towards the absorber on the distance $\lambda/2$, where λ is the wavelength of the radiation field. If the phase shift takes place at $t_1 > t_0$, the probability

amplitude of the photon is described by the equation, see Refs. [10, 11],

$$a_\pi(t) = [\Theta(t - t_0) - 2\Theta(t - t_1)]e^{-(i\omega_s + \gamma)(t - t_0)}. \quad (20)$$

The Fourier transform of its amplitude $a_{\pi 0}(t) = a_\pi(t) \exp[i\omega_s(t - t_0)]$ is

$$A_{\pi 0}(\nu) = \frac{1 - 2e^{-(\gamma - i\nu)(t_1 - t_0)}}{\gamma - i(\nu + \Delta)}. \quad (21)$$

Obviously, such a phase shift changes the photon spectrum, introducing oscillations with a period $(t_1 - t_0)/2\pi$.

Substituting $A_{\pi 0}(\nu)$ into Eq. (2) instead of $A_0(\nu)$ and calculating the integral, we obtain the expression for the amplitude of the output radiation field

$$a_\pi(l, t) = a(l, t) - 2a(l, t - t_1)e^{-\gamma t_1 - i\omega_s t_1}, \quad (22)$$

where $t_0 = 0$ and $a(l, t)$ is defined by Eq. (2) where the photon spectral function is $A_0(\nu)$. Eq. (22) coincides with that found in Ref. [10] for the output radiation field if the input field experiences the π -phase shift.

A. Resonant case

In resonant case ($\Delta = 0$) Eq. (22) simplifies as follows

$$a_\pi(l, t) = a(t) \left[J_0(2\sqrt{bt}) - 2\Theta(t - t_1) J_0(2\sqrt{b(t - t_1)}) \right]. \quad (23)$$

At $t = t_1$ it has a sharp peak whose amplitude $a_{\pi 0}(t, l) = a_\pi(t, l)e^{+i\omega_s t + \gamma t}$ is

$$a_{\pi 0}(l, t_1) = J_0(2\sqrt{bt_1}) - 2. \quad (24)$$

The corresponding probability $p_{\pi 0}(l, t) = |a_{\pi 0}(l, t)|^2$ is

$$p_{\pi 0}(l, t_1) = \left[J_0(2\sqrt{bt_1}) - 2 \right]^2. \quad (25)$$

The amplitude $a_{\pi 0}(t, l)$ and the probability $p_{\pi 0}(l, t)$ are defined without the exponential factors $\exp(-\gamma t)$ and $\exp(-2\gamma t)$, respectively, to visualize their comparison with the amplitude and probability of the input radiation field, which are unity without these factors for any t_1 .

Below, for simplicity of notations we introduce the parameter $\Gamma = 2\gamma$, which is the decay rate of the probability of the incident photon. Neglecting the Bessel function in the equation

(25) we find that the total probability $p_\pi(l, t) = |a_\pi(l, t)|^2$ increases four times with respect to its value $\exp(-\Gamma t_1)$ with no absorber between the source and the detector.

Meanwhile, the Bessel function $J_0(2\sqrt{bt})$ has a first minimum with negative value -0.403 when $bt_1 \simeq 3.67$. Therefore, at t_1 , satisfying this relation, $p_\pi(l, t_1)$ increases even more, i.e., 5.77 times with respect to the probability of the incident photon $p(t_1)$, see Ref. [10]. The time dependence of the probability $p_\pi(l, t)$ if $bt_1 \simeq 3.67$ is shown in Fig. 1a.

It is obvious that due to the π phase-shift the absorption of the photon is decreased. To calculate the total value of the transmitted radiation before and after phase shift we recall that for a classical field, the total energy, transmitted through a unit area of the absorber of thickness l , is proportional to

$$n(l, \Delta) = \int_{-\infty}^{+\infty} a(l, t) a^*(l, t) dt, \quad (26)$$

For a single photon, this value is proportional to the number of counts of the second detector in a wide time window without use of the first detector. Substituting $a(l, t)$ from Eq. (2) into Eq. (26) and calculating two integrals we obtain

$$n(l, \Delta) = \int_{-\infty}^{+\infty} \Phi_0(\nu) e^{-2\text{Re}[\alpha(\nu)]l} d\nu, \quad (27)$$

where $\Phi_0(\nu) = A_0(\nu) A_0^*(\nu)/2\pi$ is the energy spectral density of the incident radiation field. In resonance for the phase-shifted photon the time integrated probability is

$$n_\pi(T) = \int_{-\infty}^{+\infty} \Phi_\pi(\nu) e^{-2\text{Re}[\alpha(\nu)]l} d\nu, \quad (28)$$

where $\Phi_\pi(\nu) = A_{\pi 0}(\nu) A_{\pi 0}^*(\nu)/2\pi$ is the energy spectrum of the radiation field, which is

$$2\pi\Phi_\pi(\nu) = \frac{1 + 4(e^{-2\gamma t_1} - e^{-\gamma t_1} \cos \nu t_1)}{\nu^2 + \gamma^2}, \quad (29)$$

and $\alpha(\nu)$ is defined in Eq. (5), where $\Delta = 0$. The time integrated probability of the photon without phase shift for $\Delta = 0$ is (see Refs. [23, 27, 32])

$$n(l, 0) = e^{-\alpha_B l/2} I_0(\alpha_B l/2) n_0, \quad (30)$$

where $n_0 = n(0, 0) = 1/\Gamma$ and $I_0(\alpha_B l/2)$ is the modified Bessel function of zero order. For large optical thickness ($T \gg 1$) the transmitted intensity decreases as $n(l, 0) \approx n_0/\sqrt{\pi\alpha_B l}$, see Ref. [23, 27, 33]. This dependence deviates strongly from the Beer's law, $\exp(-\alpha_B l)$,

for the monochromatic radiation because of low absorption of the long wings of the input radiation field spectrum $\Phi_0(\nu)$.

A comparison of the thickness dependence of the absorption of the resonant photon without phase shift, $n(l, 0)$, see Eq. (30), with that for the photon with the phase shift, $n_\pi(T)$, is shown in Fig. 1b. We selected t_1 , which satisfies the relation $bt_1 \simeq 3.67$ when the burst takes the maximum probability $p_{\pi 0}(l, t_1) = 5.77$. With this relation ($bt_1 \simeq 3.67$) time $t_1 \simeq 14.67/TT$ decreases with thickness increase. From the plot 1b it is clear that for $T \approx 20$ almost 45% of the radiation is not absorbed and transmitted intensity increases ~ 3.5 times due to the phase shift.

B. Nonresonant case

If $\Delta \neq 0$ the functions $a(l, t)$ and $a(l, t - t_1)$ in Eq. (22) for the probability amplitude of the output radiation are described by Eq. (10). As it is shown in Sec. II for the nonresonant excitation the scattered field $a(t)f_{sc}(t)$ consists of two parts, i.e., the fast $a(t)f_{sc1}(t)$ and the slow $a(t)f_{sc2}(t)$ radiation fields. If the phase of the incoming field changes to π , the interference of the fast radiation with the phase shifted incoming field will produce a spike whose amplitude increases approximately two times, similar to the resonant case. Meanwhile, if by the time t_1 the slow field $a(t)f_{sc2}(t)$ is developed in the absorber, it will also contribute to the total amplitude.

The phase of the slow field is defined by the value $-b/\Delta$, see Eq. (19). If $b/\Delta = \pm\pi$, the slow field also interferes constructively with the phase shifted incoming field at $t \geq t_1$. In this case we have constructive interference of three fields, i.e., the incoming field, the fast field $a(t_1)f_{sc1}(t_1)$, and the slow field $a(t_1)f_{sc2}(t_1)$. Then, one can expect the spike whose amplitude is three times larger than the amplitude of the incoming radiation and its probability is nine times larger. The explicit expression for the amplitude $a_{\pi 0}(l, t)$ of the spike at t_1 is

$$a_{\pi 0}(l, t_1) = e^{i\Delta t_1} J_0 \left(2\sqrt{bt_1} \right) + f_{sc2}(t_1) - 2. \quad (31)$$

Definite conditions should be fulfilled in order the field $a(t_1)f_{sc2}(t_1)$ could develop until time t_1 to give an appreciable contribution to the total field. The thicker the absorber, the shorter time t_1 is. Also, with Δ increase the time of the slow field development shortens. This point is illustrated in Fig. 2a, where the dependence of the maximum probability of the burst,

$p_{\pi 0}(l, t_1)$, on the detuning Δ is shown for $T = 26$ and different times t_1 .

For $\Gamma t_1 = 5$ (shown by solid line on the plot) the slow field has time to reach its maximum amplitude and hence the maximum probability takes place if $\Delta = \pm 2.14\Gamma$. For these values of the detuning Δ the slow field has the phase $b/\Delta = \pm 3.037$, which is close to $\pm\pi$. This is just the condition for the constructive interference of the input field with the slow field. For $\Gamma t_1 = 5$ the contribution of the term $\exp(i\Delta t_1)J_0(2\sqrt{bt_1})$ to the amplitude of the fast field, $a(t)f_{sc1}(t)$, is almost negligible, see Eq. (13).

For the shorter time, $\Gamma t_1 = 2$ (shown by dotted line in Fig. 2a), the amplitude of the slow field does not reach its maximum value, however for $\Delta = \pm 2.6\Gamma$ the slow field has a proper phase (close to $\pm\pi$) to interfere constructively with the input radiation at $t = t_1$. With further increase of $|\Delta|$ the amplitude of the slow field also increases but the absolute value of its phase, $|b/\Delta|$, decreases to zero. Therefore, for large $|\Delta|$ the real part of the amplitude of the slow field interferes destructively with the input radiation, while its imaginary part gives some contribution to the probability $p_{\pi 0}(l, t_1)$. As a result, the maximum value of the probability of the burst becomes smaller than 4. Besides, the part, $\exp(i\Delta t_1)J_0(2\sqrt{bt_1})$, of the fast field, $a(t)f_{sc1}(t)$, contributes to the signal at t_1 . Its phase depends on the value of bt_1 due to the oscillations of the Bessel function and on the value of Δt_1 due to the exponent. The time evolution of the photon probability $p_{\pi}(l, t_1)$ for $\Gamma t_1 = 2$ and $T = 26$ is shown in Fig. 2b, where solid line represents the time dependence of the probability when the detuning is $\Delta = 2.6\Gamma$ and dotted line is for $\Delta = 0$. Appreciable increase of the amplitude of the spike for $\Delta = 2.6\Gamma$ with respect to the resonant case, $\Delta = 0$, is clearly seen.

For even shorter time, $\Gamma t_1 = 0.5$ (shown by dash-dotted line in Fig. 1a), the slow field has no time to develop for the detunings $|\Delta| \lesssim 6\Gamma$. For large detunings, $|\Delta| \gtrsim 6\Gamma$, the slow field is developed to a certain extent, but the absolute value of its phase becomes appreciably smaller than π and hence the slow field interferes destructively with the phase shifted incoming field. The part, $\exp(i\Delta t_1)J_0(2\sqrt{bt_1})$, of the fast field also changes its phase due to the exponential factor to the value Δt_1 , which is close to $\pm\pi$ for $\Delta = \pm 6\Gamma$, while $J_0(2\sqrt{bt_1})$ is negative and its value is close to the first minimum of the Bessel function. Thus, the value of product $\exp(i\Delta t_1)J_0(2\sqrt{bt_1})$ is positive. Therefore, the interference of the slow field, the part of the fast field, and the phase shifted incoming field, becomes destructive, which results in the decrease of the probability $p_{\pi 0}(l, t_1)$ with $|\Delta|$ increase.

For the absorber with a moderate thickness the interference of the three fields produces

the radiation burst whose probability does not reach its maximum value of 10. However its probability can be larger than that for the resonant excitation when the slow field is not developed at all. For example, in the absorber with optical thickness $T = 12$ the probability of the radiation burst for the nonresonant excitation is still larger than that one can observe for the resonant excitation if the condition of the maximum amplitude of the burst, $bt_1 \simeq 3.67$, is satisfied, see Fig. 3a. Comparison of the time dependence of $p_\pi(l, t)$ for resonant excitation (dotted line) and nonresonant excitation (solid line), when the phase shift takes place in both cases at the same time $t_1 = 2.5/\Gamma$, is shown in Fig. 3b.

Another interesting feature of the interference of the three fields is the possibility of their destructive interference, which is seen as a radiation quenching. It takes place for large resonant detuning Δ when the phase of the slow field is close to zero while the phase shifted incoming field has phase π . This case is illustrated in Fig. 4 where time dependence of the detection probability $p_\pi(l, t)$ of the radiation with resonant detuning $\Delta = 4\Gamma$ at the output of the absorber with optical thickness $T = 12$ is shown if at time $t_1 = 2/\Gamma$ input radiation changes its phase to π .

Just after the phase shift the radiation burst is almost negligible since the slow field, $a_{sl}(t)$, and the input field are in antiphase, and they nearly compensate each other. Mostly, the fast radiation, $a_{fs}(t)$, which is not compensated at t_1 , contributes to the output field. However, after some short time after t_1 a new fast field is generated, which compensates the previously generated fast field $a_{fs}(t)$. Due to their destructive interference the dip in the time dependence of $p_\pi(l, t)$ is developed.

Destructive echo signals in the nuclear resonant scattering of synchrotron radiation on two absorbers, the position of one of which is modulated with respect to the other, were also found in Ref. [14]. The dip in the time dependence of the probability of scattered radiation is observed if the second absorber was $5 \div 7$ times thicker than the first absorber.

IV. INSTANTANEOUS FREQUENCY SHIFT OF THE INCIDENT RADIATION FIELD

Instantaneous phase shift of the radiation field is practically impossible. If, for example, the radiation source suddenly changes its position with respect to the absorber, physically this change takes a finite time to be performed. For simplicity we assume that at time

t_1 the source starts to move with constant velocity v and it stops at time t_2 . This is also idealization, since the source cannot acquire finite velocity v instantly, and it cannot stop instantly. However, this idealization helps to understand physical processes in the experiment with suddenly moving source or absorber.

Radiative decoupling and coupling of nuclei by stepwise Doppler-energy shift was studied for two absorbers, excited by synchrotron radiation, in Ref. [14]

According to the model with constant velocity the phase factor $\exp(ikr)$ of the radiation field changes in a time interval between t_1 and t_2 as $\exp[ikr_0 + i\varphi(t)]$, where k is the wave number, r_0 is position of the source with respect to the absorber at time t_1 , and $\varphi(t) = kvt$, which we express as follows

$$\varphi(t) = \delta\omega [(t - t_1)\Theta(t - t_1) - (t - t_2)\Theta(t - t_2)]. \quad (32)$$

Here $\delta\omega$ has a meaning of the instantaneous frequency shift of the input radiation to the constant value lasting from time t_1 to t_2 . It can be expressed as $\delta\omega = \delta\varphi/\tau_v$, where $\delta\varphi$ is a total phase shift, which takes place in a time interval $\tau_v = t_2 - t_1$. The parameters $\delta\omega$, $\delta\varphi$, and τ_v play a crucial role in the effectiveness of the phase shift.

Generally, if $\varphi(t)$ has an arbitrary time dependence, the probability amplitude of the input radiation field can be expressed as $a_\varphi(t) = a(t) \exp[i\varphi(t)]$. To calculate the probability amplitude of the radiation field at the output of the absorber we use Eq. (7) in a form

$$a_\varphi(l, t) = e^{-i\omega_s t} \int_{-\infty}^{+\infty} a_0(t - \tau) e^{i\varphi(t - \tau)} R(\tau) d\tau, \quad (33)$$

which is valid due to the convolution theorem. Taking into account the definition of the response function $R(\tau)$ of the absorber, Eq. (8), and calculating the integral in Eq. (33) we obtain

$$a_\varphi(l, t) = a(t) \left[J_0 \left(2\sqrt{bt} \right) e^{i\Delta t + i\varphi(0)} + f_\varphi(t) \right], \quad (34)$$

$$f_\varphi(t) = i \int_0^t [\varphi'_t(t - \tau) - \Delta] J_0 \left(2\sqrt{b\tau} \right) e^{i\varphi(t - \tau) + i\Delta\tau} d\tau, \quad (35)$$

where $\varphi'_t(t - \tau)$ is a time derivative of the function $\varphi(t - \tau)$.

Below we consider the model with constant velocity of the source in a time interval τ_v . We study the case if $\delta\omega \gg b$. If the frequency shift $\delta\omega$ is comparable or smaller than b , the phase shift $\delta\varphi$ is not rapid with respect to the dynamical beats originating from the interference of the fields produced in a multiple scattering of the incoming radiation. Thus,

such a slow phase shift cannot strongly compete with this interference and produce a sharp burst of the radiation field.

If $\delta\varphi = \pi$ and $b\tau_v \ll 1$, with the help of Eqs. (34),(35) one can show that the model with constant velocity gives the same result as the model with the instantaneous phase shift where $\tau_v = 0$. If the product $b\tau_v$ is comparable with unity or larger than unity, the phase shift of the field can produce an essential burst of the radiation if $\delta\varphi \gg \pi$. To prove this we consider the resonant ($\Delta = 0$) and nonresonant ($\Delta \neq 0$) excitation separately.

A. Resonant excitation

To calculate the integral in Eq. (35) we consider a plane (t, τ) , where lines $t = \tau$, $t - t_1 = \tau$, and $t - t_2 = \tau$ divide this plane in three domains important for the integration, i.e. I, II, and III, see Fig. 5. In the domain I we have $t - t_1 < \tau$ or $t - \tau < t_1$ and hence $\varphi(t - \tau) = 0$. In the domain II the inequality $t_1 < t - \tau < t_2$ holds and hence $\varphi(t - \tau) = \delta\omega(t - t_1 - \tau)$. In the domain III we have $t_2 < t - \tau$ and hence the function $\varphi(t - \tau)$ has again zero value. Thus, the integral in Eq. (35) is zero in the domains I and III and it gives nonzero contribution only in the domain II. According to these arguments the integral is zero for $t < t_1$ and it has nonzero value for $t \geq t_1$.

The domain II, in its turn, can be divided in two subdomains. One subdomain (b) is located below the dashed arrow, shown in Fig. 5, and it corresponds to time $t_1 \leq t \leq t_2$. The other subdomain (a) is above this dashed arrow and it corresponds to time $t > t_2$. For the subdomain (b), where $t_1 \leq t \leq t_2$, the integral in Eq. (35) is reduced to

$$f_b(t) = i\delta\omega \int_0^{t-t_1} e^{i\delta\omega(t-t_1-\tau)} J_0(2\sqrt{b\tau}) d\tau. \quad (36)$$

If $\delta\omega \gg b$, this integral can be calculated by parts iteratively. Retaining only terms not smaller than $b/\delta\omega$, we obtain

$$f_b(t) \approx e^{i\delta\omega(t-t_1)} - J_0\left[2\sqrt{b(t-t_1)}\right] + i\frac{b}{\delta\omega} \left\{ e^{i\delta\omega(t-t_1)} - \frac{J_1\left[2\sqrt{b(t-t_1)}\right]}{\sqrt{b(t-t_1)}} \right\}. \quad (37)$$

If $bt_1 \gg 1$ we can neglect in $a_\varphi(l, t)$, Eq. (35), the term proportional to the Bessel function $J_0(2\sqrt{bt})$. Then, neglecting corrections proportional to $b/\delta\omega$ in Eq. (37) we obtain the following approximation for the probability of the radiation field, $p_\varphi(l, t) = |a_\varphi(l, t)|^2$, i.e.,

its phase dependent part $p_{\varphi 0}(l, t) = p_{\varphi}(l, t) / |a(t)|^2$,

$$p_{\varphi 0}(l, t) \approx 1 + J_0^2 \left[2\sqrt{b(t-t_1)} \right] - 2 \cos [\delta\omega(t-t_1)] J_0 \left[2\sqrt{b(t-t_1)} \right]. \quad (38)$$

which is valid for $t_1 \leq t \leq t_2$. This probability has a first maximum at $\delta\omega(t-t_1) = \pi$. If $\delta\varphi = \delta\omega(t_2-t_1) = \pi$ and $b(t_2-t_1) \ll 1$, such an instantaneous frequency shift gives the same burst whose maximum is 4 as in the case of the instantaneous phase shift [compare with Eq. (25)]. If $\delta\omega(t_2-t_1) \gg \pi$, the maxima take place at $\delta\omega(t-t_1) = (2m+1)\pi$ where m is a natural number. Their values are

$$p_{\varphi 0}(l, t) \approx \left\{ 1 + J_0^2 \left[2\sqrt{(2m+1)\pi b/\delta\omega} \right] \right\}^2. \quad (39)$$

The minima of $p_{\varphi 0}(l, t)$,

$$p_{\varphi 0}(l, t) \approx \left\{ 1 - J_0^2 \left[2\sqrt{2m\pi b/\delta\omega} \right] \right\}^2, \quad (40)$$

take place at $\delta\omega(t-t_1) = 2m\pi$. Their values are close to zero if $2m\pi b/\delta\omega \ll 1$.

For the subdomain (a), where $t > t_2$, the integral in Eq. (35) is reduced to

$$f_a(t) = i\delta\omega \int_{t-t_2}^{t-t_1} e^{i\delta\omega(t-t_1-\tau)} J_0 \left(2\sqrt{b\tau} \right) d\tau. \quad (41)$$

If $\delta\omega \gg b$, this integral can be also calculated by parts iteratively. Retaining only terms not smaller than $b/\delta\omega$, we obtain

$$f_a(t) \approx e^{i\delta\varphi} f(t-t_2) - f(t-t_1), \quad (42)$$

where

$$f(t) = J_0 \left(2\sqrt{bt} \right) + i \frac{b}{\delta\omega} \cdot \frac{J_1 \left(2\sqrt{bt} \right)}{\sqrt{bt}}. \quad (43)$$

With the definition (43) the function $f_b(t)$ in Eq. (37) can be expressed as

$$f_b(t) \approx e^{i\delta\omega(t-t_1)} f(0) - f(t-t_1). \quad (44)$$

The first term, in this expression can be interpreted as the frequency shifted incoming field and the second term as the scattered radiation field. Depending on the value of the phase factor $\delta\omega(t-t_1)$ these fields interfere destructively or constructively.

Combining the results of the calculation of the integral in the domains I-III, we obtain the final expression for the probability amplitude of the output radiation

$$a_{\varphi}(l, t) = a(t) \left\{ J_0 \left(2\sqrt{bt} \right) + \Theta(t-t_1) f_b(t) + \Theta(t-t_2) [f_a(t) - f_b(t)] \right\}. \quad (45)$$

Comparison of the time evolution of the spike after the instantaneous phase shift to π (bold solid line) and during the instantaneous frequency shift (thin solid line) is shown in Fig. 6. It is clearly seen from the plot that the burst in the second case consists of two maxima. The positions of the maxima and minimum are well described by simple relations, i.e., $\delta\omega(t - t_1) = \pi$ and $\delta\omega(t - t_1) = 3\pi$ for the maxima, and $\delta\omega(t - t_1) = 2\pi$ for the minimum. The spike in the second case has reduced intensity and broadened with respect to the spike in the case of the instantaneous phase shift. The probability $p_\varphi(l, t)$, calculated with the help of the approximate expressions for $f_a(t)$, Eq. (42), and $f_b(t)$, Eq. (44), is shown by dots. For $\delta\varphi = 10$ radian, $\Gamma\tau_v = 0.3$, $\delta\omega = 33.3\Gamma$, and $b = 3\Gamma$ the results of the numerical calculation of the integral and analytical approximations are indistinguishable. It should be noted that in this example the product $b\tau_v = 0.9$ is close to unity.

B. Nonresonant excitation

For the nonresonant excitation the integral in Eq. (35) is not zero in all three domains, I, II, and III, see Fig. 5.

In a time interval between $t = 0$ and $t = t_1$ this integral is $f_\varphi(t) = f_{\text{Ib}}(t)$ where

$$f_{\text{Ib}}(t) = -i \int_0^t \Delta J_0 \left(2\sqrt{b\tau} \right) e^{i\Delta\tau} d\tau, \quad (46)$$

and index Ib denotes that the integral is taken in the domain I, subdomain b, which is located below the dash-dotted line in Fig. 5. This integral coincides with $f_{sc2}(t)$ in Eq. (14).

In a time interval $t_1 \leq t \leq t_2$ this integral is $f_\varphi(t) = e^{i\delta\omega(t-t_1)} f_{\text{IIb}}(t - t_1) + f_{\text{Ia}}(t)$, where

$$f_{\text{IIb}}(t - t_1) = -i \int_0^{t-t_1} (\Delta - \delta\omega) J_0 \left(2\sqrt{b\tau} \right) e^{i(\Delta - \delta\omega)\tau} d\tau, \quad (47)$$

$$f_{\text{Ia}}(t) = -i \int_{t-t_1}^t \Delta J_0 \left(2\sqrt{b\tau} \right) e^{i\Delta\tau} d\tau. \quad (48)$$

Here index IIb in $f_{\text{IIb}}(t)$ denotes that the integral is taken in the domain II, subdomain b, which is located below the dashed line in Fig. 5, and index Ia in $f_{\text{Ia}}(t)$ denotes that the integral is taken in the domain I, subdomain a, which is located above the dash-dotted line.

For $t > t_2$ this integral is $f_\varphi(t) = f_{\text{III}}(t) + e^{i\delta\omega(t-t_1)} f_{\text{IIa}}(t) + f_{\text{Ia}}(t)$, where

$$f_{\text{III}}(t) = -i \int_0^{t-t_2} \Delta J_0 \left(2\sqrt{b\tau} \right) e^{i(\Delta\tau + \delta\varphi)} d\tau. \quad (49)$$

$$f_{\text{IIa}}(t) = f_{\text{IIb}}(t - t_1) - f_{\text{IIb}}(t - t_2). \quad (50)$$

Here index III in $f_{\text{III}}(t)$ denotes that the integral is taken in the domain III in Fig. 5, and index IIa in $f_{\text{IIa}}(t)$ denotes that the integral is taken in the domain II, subdomain a, which is located above the dashed line.

With these definitions the integral in Eq. (35) can be written as

$$f_\varphi(t) = F_1(t) + F_2(t), \quad (51)$$

$$F_1(t) = f_{sc2}(t) - \Theta(t - t_1)f_{sc2}(t - t_1) + \Theta(t - t_2)e^{i\delta\varphi}f_{sc2}(t - t_2), \quad (52)$$

$$F_2(t) = e^{i\delta\omega(t-t_1)}[\Theta(t - t_1)f_{\text{IIb}}(t - t_1) - \Theta(t - t_2)f_{\text{IIb}}(t - t_2)]. \quad (53)$$

If $b\tau_v \ll 1$ and $\tau_v \ll t_1$, the main contribution to the function $F_1(t)$ in the time interval, when the frequency shift takes place, is given by the slow field $f_{sc2}(t)$, developed before the frequency shift.

If $\delta\omega \gg |\Delta|, b$, the function $f_{\text{IIb}}(t - t_1)$ can be calculated by parts iteratively. Retaining only terms not smaller than $b/(\delta\omega - \Delta)$, we obtain

$$f_{\text{IIb}}(t - t_1) \approx f_\Delta(0) - e^{i(\Delta - \delta\omega)(t-t_1)}f_\Delta(t - t_1), \quad (54)$$

where

$$f_\Delta(t) = J_0(2\sqrt{bt}) + i\frac{b}{\delta\omega - \Delta} \cdot \frac{J_1(2\sqrt{bt})}{\sqrt{bt}}. \quad (55)$$

In a time interval $0 < t < t_2$ the function $f_\varphi(t)$, Eq. (35), is approximated as follows

$$f_\varphi(t) \approx F_1(t) + \Theta(t - t_1)[e^{i\delta\omega(t-t_1)}f_\Delta(0) - e^{i\Delta(t-t_1)}f_\Delta(t - t_1)]. \quad (56)$$

If during the frequency shift ($t_1 < t < t_2$) all three components of this function are in phase they interfere constructively, what is seen as a burst of the radiation field. For example, the first spike takes place if the first term $F_1(t) \approx f_{sc2}(t)$, describing the slow field, is negative and it has maximum absolute value, the second term is negative if $\delta\omega(t - t_1) = \pi$, and the third term is negative if $\Delta(t - t_1) \ll 1$.

For $t > t_2$ with the same approximations the function $f_\varphi(t)$ is

$$f_\varphi(t) \approx F_1(t) + e^{i\Delta(t-t_2)+i\delta\varphi}f_\Delta(t - t_2) - e^{i\Delta(t-t_1)}f_\Delta(t - t_1). \quad (57)$$

The time dependence of the detection probability of the radiation field, $p_\varphi(l, t)$, calculated with the help of Eq. (34), where $f_\varphi(t)$ is approximated by equations (56) and (57), is shown

in Fig. 7 by solid line. For the parameters $\delta\varphi = 10$ radian, $b = 3\Gamma$, $t_1 = 2.4/\Gamma$, and $\tau_v = 0.3/\Gamma$ this approximation is indistinguishable from the exact result, Eq. (34), where the function $f_\varphi(t)$, Eq. (35), is calculated numerically. Two plots are represented in Fig. 7. One (solid line) is for $\Delta = 1.5\Gamma$ and the other (dotted line) is for the resonant excitation ($\Delta = 0$). It is clearly seen that two spikes for the nonresonant excitation are larger than for resonant excitation. As it was shown in the previous subsection, for the resonant excitation the first maximum of the burst takes place at $t = t_1 + \pi/\delta\omega$. For the nonresonant case it takes place slightly later, i.e., at $t = t_1 + \pi/(\delta\omega - \Delta)$ if $\Delta > 0$, or earlier if $\Delta < 0$.

V. EXPERIMENT

Our experimental setup is based on an ordinary delayed coincidence scheme usually used in measurements of the lifetimes of nuclear states. The schematic arrangement of the source, absorber, detectors, and electronics is shown in Fig. 8. The source, $^{57}\text{Co}:\text{RH}$, is mounted on the holder of the Mössbauer drive, which is used to Doppler shift the frequency of the radiation of the source. The details of this setup are described in Ref. [30]. The only difference is in the holder for the absorber and some additional electronics.

The absorber was made of enriched $\text{K}_4\text{Fe}(\text{CN})_6 \cdot 3\text{H}_2\text{O}$ powder with effective thickness of 13.2. It was glued on a polyvinylidene fluoride (PVDF) piezo polymer transducer (thickness $28\text{ }\mu\text{m}$, model LDT0-28K, Measurement Specialties, Inc.). Several piezoelectric transducer constructions were tested to achieve controlled phase change of the radiation field. The best of them was a piece of $28\text{ }\mu\text{m}$ thick, $3 \times 5\text{ mm}$ polar PVDF film coupled to a plexiglas backing of $\sim 2\text{ mm}$ thickness with epoxy glue. The PVDF film was driven with a square wave pulse from Ortec Gate&Delay Generator (Model 416A) or Mini-Circuits Model ZPUL-21 Pulse Amplifier. They were triggered by the positive/negative output of the 122 keV channel constant fraction discriminator. The rise time of the driving pulse was about 18 nsec and 10 nsec for Gate&Delay Generator and Pulse Amplifier, respectively.

To calibrate a time resolution of our setup we measured a time spectrum of the decay of 14.4 keV state with no absorber. The time resolution of 9.1(5) nsec was obtained by least square fitting the experimental lifetime spectra with the convolution of the theoretical decay curve and a Gaussian distribution originating from the time resolution function of the experimental setup (see, for example, Ref. [35] for the procedure). The curve measured for

a single line source ^{57}Co shows the single exponential decay with a mean life time $\tau_{lt} = 1/\Gamma$ of 140(9) nsec, in good agreement with the mean lifetime and the natural linewidth data for the 14.4 keV state of ^{57}Fe .

Our experimental results of measurements of time dependence of the transmission through the absorber with effective thickness of 13.2 are shown in Fig. 9. Different detunings Δ are obtained by Doppler shift the radiation frequency of the source with respect to the resonant frequency of the absorber. In Figs. 9a-9d and Fig. 9e voltage steps +10V and -4 V, respectively, were applied across the transducer at time $t_1 - t_0 \simeq 280$ nsec. In Fig. 9f a voltage step +10V was applied at time $t_1 - t_0 \simeq 140$ nsec.

In Fig. 9 the background due to accidental coincidences and the fraction of radiation with recoil, which is nonresonant for the absorber, are subtracted from data. The background is defined from the counting rate at times preceding the fast front of the incident radiation pulses. A contribution from the radiation field with recoil is estimated as follows. Theoretical prediction of its contribution to the radiation probability is $p_{nr}(t) = (1 - f_s)p(t)$. Then, the total probability of the radiation at the output of the resonant absorber is $p_{tot}(t) = p_{nr}(t) + f_s p(l, t)$, where $p(l, t) = |a(l, t)|^2$ is the contribution from resonant photons without recoil. The convolution of the function $p_{tot}(t)$ with the Gaussian distribution, responsible for the time resolution of our setup, is proportional to the time dependence of the number of counts $N(t)$, measured in the experiment. Fitting the experimental time spectra to the theoretical time dependence of $N(t)$ with and without absorber, in resonance and far from resonance we obtained $f_s = 0.75(9)$, which is consistent with the value f_s reported in previous publications (see, for example, Ref. [36]). These measurements were done without voltage steps. Photons, emitted with recoil, pass through the absorber with no change since they are not resonant for ^{57}Fe nuclei. Therefore these photons carry no information about the absorber and their contribution to the detector counts can be safely removed from the data.

VI. DISCUSSION

The experimental results were fitted with a full theoretical expression based on Eqs. (34), (35). The shape of the phase function $\varphi(t)$ was obtained by computer fitting the experimental data. Actually we derived a function describing the charge collection on each conducting plate of the PVDF transducer, which form a capacitor. We calculated a voltage,

which is created across the plates of the capacitor by the voltage step applied from the external source to the transducer. We assumed that the mechanical displacement of the transducer faces with respect to each other due to piezo effect is proportional to the voltage across the capacitor. However, such a simplified picture does not take into account the mechanical properties of the transducer. Each mechanical stress of the transducer creates a current producing a voltage, i.e., so called charge generator is to be present in the model of the piezo transducer on the top of the capacitor, formed by the conducting plates. Therefore, in our imperfect model of the phase function the fitting parameters were not relevant to the duration of the voltage step of the source, to the capacitance of the transducer, and to the internal resistance of the voltage source. The shape of the fitting function $\varphi(t)$ is shown in Fig. 10. Its maximum value $\delta\varphi$ varies between 14 and 10 radian for experimental plots in Figs. 9 a-d and 9f, where voltage step was +10 V, and it equals -4.5 radian for Fig. 9e, where voltage step was -4 V. While it describes quite well the main part of the transient pulse, it fails to describe oscillations obviously seen in the tail of these transients.

The time dependence of $\varphi(t)$, shown in Fig. 10, explains why the transient pulses are quite extended in our experiments. We assume that mechanical displacement of the transducer slows down due to the fact that a heavy weight of the absorber affects strongly the mechanical properties of the light PVDF transducer whose density is nearly 3-4 times smaller.

The plots a-d in Fig. 9 obviously show that the amplitude of the pulse of the photon revival is larger for the nonresonant excitation ($\Delta = +1.3\Gamma$ and $\Delta = -1.4\Gamma$) compared with that for nearly resonant excitation ($\Delta = -0.05\Gamma$). With further increase of the resonant detuning ($\Delta = -1.93\Gamma$) this amplitude decreases. For large detuning ($\Delta = -2.6\Gamma$) destructive interference is observed (see Fig. 9e).

The delayed-coincidence spectrum in Fig. 9f is measured when the step voltage is applied almost two times earlier than in Fig. 9a-9e.

Thus, plots a-e qualitatively confirm our theoretical analysis of the interference of three fields. In resonance ($\Delta = 0$) the first maximum of the pulse takes place when $\varphi(t) = \pi$, while the first minimum, if observed, takes place when $\varphi(t) = 2\pi$. This allows to control the position of the absorber with an accuracy of half wavelength of γ -ray, which is $\lambda/2 = 43$ pm.

VII. CONCLUSION

We studied theoretically and experimentally the influence of the phase shift of a single photon wave packet after its leading edge on the transmission through an optically dense absorptive medium. In exact resonance a photon revival is observed if the phase shift is equal π . This revival appears due to the constructive interference of the phase shifted part of the field with the coherently scattered radiation field coming from the absorber excited at an earlier time. The source of the coherently scattered field is a coherent ringing of resonant particles in response to the incident radiation field. With no phase shift the interference of the coherently scattered field with the input radiation field is destructive, which is seen as acceleration of the radiation damping at the output of a thick absorber. Time integrated probability of the photon at the output of the absorber decreases due to this destructive interference and incoherent scattering as well. If the absorption spectrum of an individual resonant particle in the absorber and the energy spectrum of the photon are both Lorentzian with the same width, then the phase shift of the photon wave packet allows retrieval of almost 50% of the radiation at the output of a thick absorber.

If the central frequency of the photon spectrum is detuned from resonance with the absorber, the spectral components close to the central frequency are less absorbed. They interact adiabatically with the absorber forming a wave packet, which propagates with appreciably reduced group velocity. The phase of this adiabatic wave packet $\varphi_a = \alpha_B l \gamma / 2\Delta$ depends on the product of the half of the optical thickness of the absorber ($T/2$) and the ratio of the halfwidth of the absorption line γ and resonant detuning Δ . The scattered radiation does not change instantly after the phase shift of the input radiation field. If $\varphi_a = \pm\pi$, then just after the phase shift three fields interfere constructively producing a radiation burst. They are the phase shifted incident radiation field, the fast coherently-scattered-radiation field, coming from the absorber excited at an earlier time, and the slow component, developed before the phase shift.

We expect that the control of a single photon radiation field with the help of a thick resonant absorber, moving abruptly at a particular moment of time, could be promising for quantum information and quantum computing. In gamma domain this method helps to detect extremely small displacements of the absorber with an accuracy of 0.5 \AA . Therefore we expect that this technique could open new opportunities for calibration of displacements

of the tip of scanning tunneling microscopes.

VIII. ACKNOWLEDGEMENTS

This work was supported by National Science Foundation (USA), Russian Foundation for Basic Research (Grant 09-02-00206-a), Program of Presidium of RAS "Quantum physics of condensed matter", and Grant of Federal Agency on Education, Russia (No. NK - 02.740.11.0428).

IX. APPENDIX

A. Adiabatic approximation

An example of how the integral in Eq. (2) may be evaluated in the adiabatic following approximation, Ref. [27–31], will be presented here. This approximation describes that part of the output radiation field, which propagates in the absorber with slow group velocity. Below it will be shown that adiabatic method gives a nice approximation of the slow part of the scattered field and provides analytical estimates of the development rate of this field.

If the decay rate γ of the coherence of the nuclear excited and ground states in the absorber coincides with the decay rate of the probability amplitude of the source photon, we can introduce a new variable $\nu_1 = \nu + i\gamma$ in the integral (2), which corresponds to a shift of the integration axis in a complex plane. This substitution results in an exponentially decaying factor $\Theta(t) \exp(-\gamma t)$ for $a(l, t)$ in Eq. (2), which transforms to the integral

$$a(l, t) = \frac{a(t)}{2\pi} \int_{-\infty+i\gamma}^{+\infty+i\gamma} \frac{i}{\nu_1} \exp\left(-i\nu_1 t - \frac{ib}{\nu_1 + \Delta}\right) d\nu_1. \quad (58)$$

In the adiabatic following approach the transmission function $\alpha(\nu)$ in Eq. (2) is approximated by its expansion in a power series near $\nu = 0$. It was shown in Ref. [29] that to describe the propagation of the adiabatic part of the pulse for the off resonance excitation one can take only three terms of the expansion. For the transmission function in Eq. (58) this expansion is

$$\frac{ib}{\nu_1 + \Delta} \approx \frac{ib}{\Delta} \left(1 - \frac{\nu_1}{\Delta} + \frac{\nu_1^2}{\Delta^2} + \dots\right), \quad (59)$$

whose terms have the following physical meaning. The first term, ib/Δ , describes the total phase shift of the field at the output of the absorber. The second term, $-ib\nu_1/\Delta^2$, gives

a time delay of the pulse, $t_d = b/\Delta^2$, at the output caused by the reduction of its group velocity to the value

$$V_g = \frac{c}{1 + \frac{\alpha_B \gamma c}{2\Delta^2}}. \quad (60)$$

The third term of the expansion (59) describes the group velocity (delay) dispersion, Ref. [29].

To calculate the integral in Eq. (58) with the approximated transmission function (59) we calculate first the integral

$$R_s(t) = \frac{1}{2\pi} \int_{-\infty+i\gamma}^{+\infty+i\gamma} \exp \left[-i\nu_1(t-t_d) - i\frac{b}{\Delta} - i\frac{b}{\Delta^3}\nu_1^2 \right] d\nu_1, \quad (61)$$

which is

$$R_s(t) = \sqrt{\frac{\Delta^3}{4\pi b}} \exp \left[i\frac{\Delta^3}{4b}(t-t_d)^2 - i\frac{b}{\Delta} - i\frac{\pi}{4} \right]. \quad (62)$$

Then, with the help of the convolution theorem we find

$$a_{apr}(l, t) = a(t) \int_{-\infty}^{+\infty} R_s(t - \tau + t_d) \Theta(\tau - t_d) d\tau. \quad (63)$$

Integration gives

$$a_{apr}(l, t) = \frac{a(t)}{2} e^{-ib/\Delta} \{1 + (1-i) [C(\Delta_{br}(t-t_d)) + iS(\Delta_{br}(t-t_d))]\}, \quad (64)$$

where $C(x)$ and $S(x)$ are Fresnel integrals, Ref. [33], and $\Delta_{br} = \sqrt{\Delta^3/2\pi b}$ is a parameter, which describes the pulse broadening in time due to the group velocity dispersion.

The probability $p(l, t)$, calculated with the help of the approximation, Eq. (64), is compared in Figs. 11 and 12 with that, which is calculated with the help of the exact expression (10), for different values of the detuning Δ and b . The adiabatic approximation describes quite well time evolution of the photon probability for large t . Initial fast oscillatory decay of the photon probability is not described by this approximation. We conclude that this approximation can be used for the estimation of the development rate of slow part of the radiation field developed in the absorber.

According to the adiabatic approximation the front of the photon wave packet experiences the time delay $t_d = b/\Delta^2$ due to the reduced group velocity. The delay time t_d rises with increase of the absorber thickness, which is proportional to b . With increase of the absolute value of the detuning Δ the delay time t_d shortens. The front of the photon wave packet also experiences a time broadening due to the group velocity (delay) dispersion. The time

broadening t_{br} is quantified by a parameter $1/\Delta_{br} = \sqrt{2\pi b}/\Delta^3$. Thus, a time when the probability of the output photon reaches its input value, i.e., when the slow part of the photon wave packet is formed, can be estimated as $t_d + t_{br}$. For the numerical examples, given in Figs. 11 and 12, this estimate coincides quite well with time when $|a_{apr}(l, t)|^2$ reaches the value of $|a(t)|^2$, shown by a thin solid line. In Fig.11 this time is 24.3 (a), 7.3 (b), and 2.3 (c) in units $1/\Gamma$. In Fig.12 this time is 41.4 (a), 12.1 (b), and 3.7 (c) in units $1/\Gamma$.

Concluding this subsection we compare the time development of the absolute values of the effective amplitude of the full scattered field $f_{sc}(t)$, of the fast component $f_{sc1}(t)$ and of the slow component $f_{sc2}(t)$. Their time dependencies are shown in Fig. 13 for $b = 3\Gamma$ and $\Delta = \Gamma$ when these fields are almost in phase for large t since $b/\Delta \approx \pi$. It is clearly seen that the fast component develops really fast compared with the slow component, which reaches its maximum value with an appreciable delay.

B. Frequency domain arguments

To explain the difference in the development rates of the fast $a_{fs}(t)$ and slow $a_{sl}(t)$ components of the scattered field we address to the arguments of the concept that considers the absorber as a frequency filter, Ref. [27, 30]. First, we express the field as a sum of resonant $a_r(t)$ and nonresonant $a_{nr}(t)$ components, i.e.,

$$a(t) = a_r(t) + a_{nr}(t), \quad (65)$$

where $a_r(t) = \Theta(t) \exp(-\gamma t - i\omega_a t)$ and $a_{nr}(t) = \Theta(t) \exp(-\gamma t) [\exp(-i\omega_s t) - \exp(-i\omega_a t)]$. The amplitude $a_{r0}(t) = \Theta(t) \exp(-\gamma t + i\Delta t)$ of the field $a_r(t)$ has sharply rising leading edge, while the amplitude $a_{nr0}(t) = \Theta(t) \exp(-\gamma t) [1 - \exp(i\Delta t)]$ of the field $a_{nr}(t)$ rises smoothly with the rate Δ . Therefore, the former acquires large amplitude transients at the output of a thick absorber, and the latter develops smoothly if $b > |\Delta|$.

To show this, we calculate the Fourier transform of the components $a_{r0}(t)$ and $a_{nr0}(t)$, which are

$$A_{r0}(\nu) = \frac{i}{\nu + \Delta + i\gamma}, \quad (66)$$

$$A_{nr0}(\nu) = \frac{i\Delta}{(\nu + i\gamma)(\nu + \Delta + i\gamma)}, \quad (67)$$

respectively. The integral in Eq. (2) for the component $A_{r0}(\nu)$, describing the transmission of the resonant component through the absorber, is easily calculated. It is

$$a_{r0}(l, t) = \Theta(t)e^{-\gamma t + i\Delta t} J_0(2\sqrt{bt}), \quad (68)$$

which coincides with $[1 + f_{sc1}(t)]a_0(t)$.

For the nonresonant component $A_{nr0}(\nu)$ this integral can be calculated as follows. Since $A_{nr0}(\nu)$ is a product of $A_{r0}(\nu)$ and $\Delta/(\nu + i\gamma)$, then according to the convolution theorem we have

$$a_{nr0}(l, t) = -i\Delta\Theta(t) \int_0^t e^{-\gamma(t-\tau)} a_{r0}(l, \tau) d\tau. \quad (69)$$

Here we take into account that the original function of $\Delta/(\nu + i\gamma)$ is $-i\Delta\Theta(t)\exp(-\gamma t)$. Thus, the nonresonant component, transmitted through the absorber, $a_{nr0}(l, t)$ coincides with the slow component of the scattered field $a_{sl}(t)$.

To explain the difference in the transmission of the resonant and nonresonant components of the radiation field we compare their spectra. The resonant component $A_{r0}(\nu)$ has long wings decreasing as i/ν for large absolute values of ν . The spectral wings of the nonresonant component $A_{nr0}(\nu)$ decrease much faster as $i\Delta/\nu^2$. Therefore these components are very differently filtered by the resonant absorber. By our opinion this is the main feature making a crucial difference in properties of the slow and fast components of the scattered field.

As a proof of this statement we consider another decomposition of the single photon spectrum in two components, proposed in Refs. [27, 30]. We formally represent the Fourier transform of the single photon field Eq. (3) as $A_0(\nu) = A_{0s}(\nu) + A_{0a}(\nu)$, where

$$A_{0s}(\nu) = \frac{\gamma}{\nu^2 + \gamma^2}, \quad (70)$$

$$A_{0a}(\nu) = \frac{i\nu}{\nu^2 + \gamma^2}, \quad (71)$$

are the symmetric and antisymmetric parts, respectively. The first part is an even function whose wings decrease as γ/ν^2 . The second part is an odd function whose wings drop as i/ν .

The time domain counterparts of these functions are

$$a_{0s}(t) = \frac{1}{2} \exp(-\gamma |t|), \quad (72)$$

$$a_{0a}(t) = \begin{cases} \frac{1}{2} \exp(-\gamma t) & \text{if } t > 0, \\ 0 & \text{if } t = 0, \\ -\frac{1}{2} \exp(\gamma t) & \text{if } t < 0. \end{cases} \quad (73)$$

The function $a_{0s}(t)$ has no discontinuity, except a discontinuity in its slope. The function $a_{0a}(t)$ is a discontinuous function. Therefore, the former should not acquire large amplitude transients at the output of a thick absorber, and the latter should have them.

Calculating the integral in Eq. (7) for the components $a_{0s}(t)$ and $a_{0a}(t)$ we obtain

$$a_{0s}(l, t) = \begin{cases} \frac{1}{2} [a_0(l, t) - a_{tr}(l, t)] & \text{if } t \geq 0, \\ \frac{1}{2} \exp\left(\gamma t - \frac{b}{\Gamma - i\Delta}\right) & \text{if } t \leq 0, \end{cases} \quad (74)$$

$$a_{0a}(l, t) = \begin{cases} \frac{1}{2} [a_0(l, t) + a_{tr}(l, t)] & \text{if } t > 0, \\ -\frac{1}{2} \exp\left(\gamma t - \frac{b}{\Gamma - i\Delta}\right) & \text{if } t < 0, \end{cases} \quad (75)$$

where $a_0(l, t) = a(l, t) \exp(i\omega_s t)$, $a(l, t)$ is defined in Eq. (15) and

$$a_{tr}(l, t) = \Theta(t) \left\{ e^{-\gamma t + i\Delta t} J_0\left(2\sqrt{bt}\right) - e^{\gamma t} \left[e^{-\frac{b}{\Gamma - i\Delta}} - (\Gamma - i\Delta) \int_0^t e^{(i\Delta - \Gamma)\tau} J_0\left(2\sqrt{b\tau}\right) d\tau \right] \right\}. \quad (76)$$

Time dependence of the absolute values of the amplitudes $a_{0s}(l, t)$ and $a_{0a}(l, t)$ for $b = 3\Gamma$ and $\Delta = \Gamma$ is shown in Fig. 14. These amplitudes are compared with the absolute values of input amplitudes $a_{0s}(t)$ and $a_{0a}(t)$. It should be noted that since input amplitudes differ only in sign for $t < 0$, their absolute values are identical.

The plots in Fig.14 clearly demonstrate that symmetric component is strongly absorbed. It delays in time and its shape is smoothened and not too much corrupted. This component does not show fast and strong transients. In contrast, the asymmetric part shows strong transients. In Fig. 15 these transients are compared with that of the absolute value of the total field amplitude $a_0(l, t)$. The initial sharp rise of the total field amplitude and its first stage of fast decay coincide well with the transients of the absolute value of the amplitude of the asymmetric part.

We assume that such a time dependence is defined by the far wings of the spectrum of the asymmetric component. These wings pass through the absorber, which acts as a stop-band spectral filter rejecting the frequencies close to the resonance but transmitting the far sidebands. Just the far wings define sharply rising leading edge of the field amplitude with no delay.

To give another argument of the role of the spectral wings of the photon spectrum in the initial sharp rise of the time dependence of the single photon radiation field amplitude, we remind that if in the photon spectrum $A_0 = i/(\nu + i\gamma)$ one sets $\gamma \rightarrow 0$, then its time domain

counterpart $a_0(t) = \Theta(t) \exp(-\gamma t)$ will transform simply into the step function $\Theta(t)$.

- [1] J. I. Cirac, P. Zoller, H. J. Kimble, and H. Mabuchi, Phys. Rev. Lett. **78**, 3221 (1997).
- [2] A. E. Kozhekin, K. Molmer, and E. Polzik, Phys. Rev. A **62**, 033809 (2000).
- [3] C. Liu, Z. Dutton, C. H. Behroozi, and L. V. Hau, Nature (London) **409**, 490 (2001).
- [4] D. Phillips, A. Fleischhauer, A. Mair, R. Walsworth, and M. D. Lukin, Phys. Rev. Lett. **86**, 783 (2001).
- [5] T. Chaneliere, D. N. Matsukevich, S. D. Jenkins, S.-Y. Lan, T. A. B. Kennedy, and A. Kuzmich, Nature **438** 833 (2005).
- [6] M. D. Eisaman, A. Andre, F. Massou, M. Fleischhauer, A. S. Zibrov, and M. D. Lukin, Nature **438** 837 (2005).
- [7] F. J. Lynch, R. E. Holland, and M. Hamermesh, Phys. Rev. **120**, 513 (1960).
- [8] S. M. Harris, Phys. Rev. **124**, 1178 (1961).
- [9] R. P. Feynman, R. B. Leighton, and M. Sands, *The Feynman Lectures on Physics*, Vol I (Addison-Wesley, Reading, Mass., 1963), see especially Chap. 31.
- [10] P. Helisto, I. Tittonen, M. Lippmaa, and T. Katila, Phys. Rev. Lett. **66**, 2037 (1991).
- [11] I. Tittonen, M. Lippmaa, P. Helisto, and T. Katila, Phys. Rev. B **47**, 7840 (1993).
- [12] G. V. Smirnov, U. van Bürck, J. Arthur, S. L. Popov, A. Q. R. Baron, A. I. Chumakov, S. L. Ruby, W. Potzel, and G. S. Brown, Phys. Rev. Lett. **77**, 183 (1996).
- [13] Yu. V. Shvyd'ko, T. Hertrich, U. van Bürck, E. Gerdau, O. Leopold, J. Metge, H. D. Rüter, S. Schwendy, G. V. Smirnov, W. Potzel, and P. Schindelmann, Phys. Rev. Lett. **77**, 3232 (1996).
- [14] G. V. Smirnov and W. Potzel, Hyperfine Interactions **123/124**, 633 (1999).
- [15] M. O. Scully and M. S. Zubairy, *Quantum Optics* (Cambridge, 1997), p. 208.
- [16] R. E. Holland, F. J. Lynch, G. J. Perlow, and S. S. Hanna, Phys. Rev. Lett. **4**, 181 (1960).
- [17] N. Hayashi, T. Kinoshita, I. Sakamoto, and B. Furubayashi, Nucl. Instrum. Methods **134**, 317 (1976).
- [18] E. I. Vapirev, P. S. Kamenov, D. L. Balabansky, S. I. Ormadjiev, and K. Yanakiev, Journal de Physique **44**, 675 (1983).
- [19] M. Haas, V. Hizhnyakov, E. Realo, and J. Jögi, Phys. Status Solidi **B 149**, 283 (1988).
- [20] W. C. McDermott III and G. R. Hoy, Hyperfine Interactions **107**, 81 (1997).

- [21] G. V. Smirnov, *Hyperfine Interactions* **123/124**, 31 (1999).
- [22] D. C. Burnham and R. Y. Chao, *Phys. Rev.* **188**, 667 (1969).
- [23] M. D. Crisp, *Phys. Rev. A* **1**, 1604 (1970).
- [24] Yu. Kagan, A. M. Afanas'ev, and V. G. Kohn, *J. Phys. C* **12**, 615 (1979).
- [25] I. S. Gradshteyn and I. M. Ryzhik *Table of Integrals, Series, and Products*, edited by A. Jeffrey and D. Zwillinger, (Academic Press, 2007).
- [26] D. Grischkowsky, *Phys. Rev. A* **7**, 2096 (1973).
- [27] R. N. Shakhmuratov, J. Odeurs, and P. Mandel, *Phys. Rev. A* **75**, 013808 (2007).
- [28] R. N. Shakhmuratov and J. Odeurs, *Phys. Rev. A* **77**, 033854 (2008).
- [29] R. N. Shakhmuratov and J. Odeurs, *Phys. Rev. A* **78**, 063836 (2008).
- [30] R. N. Shakhmuratov, F. Vagizov, J. Odeurs, and O. Kocharovskaya, *Phys. Rev. A* **80**, 063805 (2009).
- [31] R. N. Shakhmuratov, *J. Mod. Opt.* **57**, 1355 (2010).
- [32] A. Vértes, L. Korecz, and K. Burger, *Mössbauer Spectroscopy* (Elsevier, New York, 1979).
- [33] *Handbook of Mathematical Functions*, edited by M. Abramowitz and I. A. Stegun (Dover, New York, 1965).
- [34] P. Schindelmann, U. van Bürck, and W. Potzel, *Phys. Rev. A* **65**, 023804 (2002).
- [35] J. C. Dehaes, *Nuclear instruments and methods* **120**, 301 (1974).
- [36] J. Ball and S.J. Lyle, *Nucl. Instrum. Methods* **163**, 177 (1979).

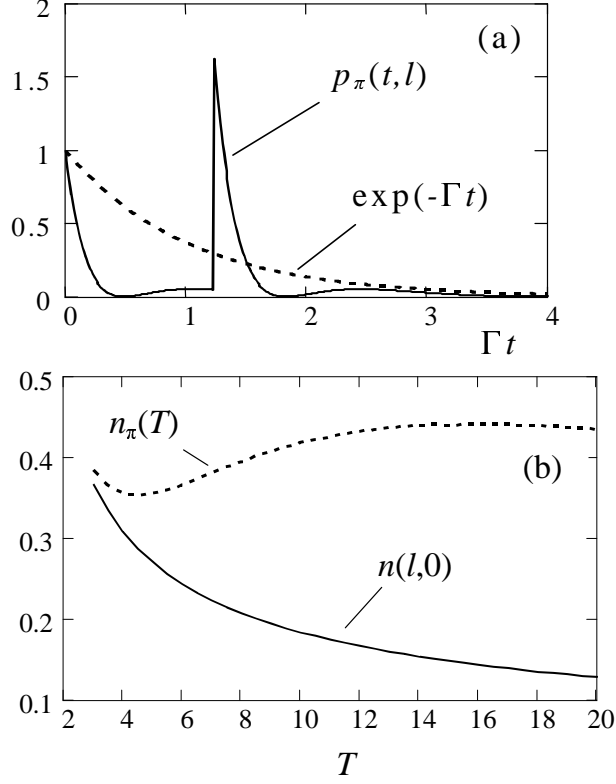


FIG. 1: (a) Time evolution of the detection probability $p_\pi(l, t)$ (solid line) of the photon at the output of the absorber with optical thickness $T = 12$, which corresponds to $b = 3\Gamma$. Time of the instantaneous phase shift, t_1 , satisfies the relation $bt_1 \simeq 3.67$, i.e., $\Gamma t_1 = 1.22$, where $\Gamma = 2\gamma$. Time evolution of the probability of the input radiation is shown by dashed line. (b) Thickness dependence of the time integrated transmission of the phase shifted photon (dashed line) and a photon without the phase shift (solid line). Both are normalized to n_0 .

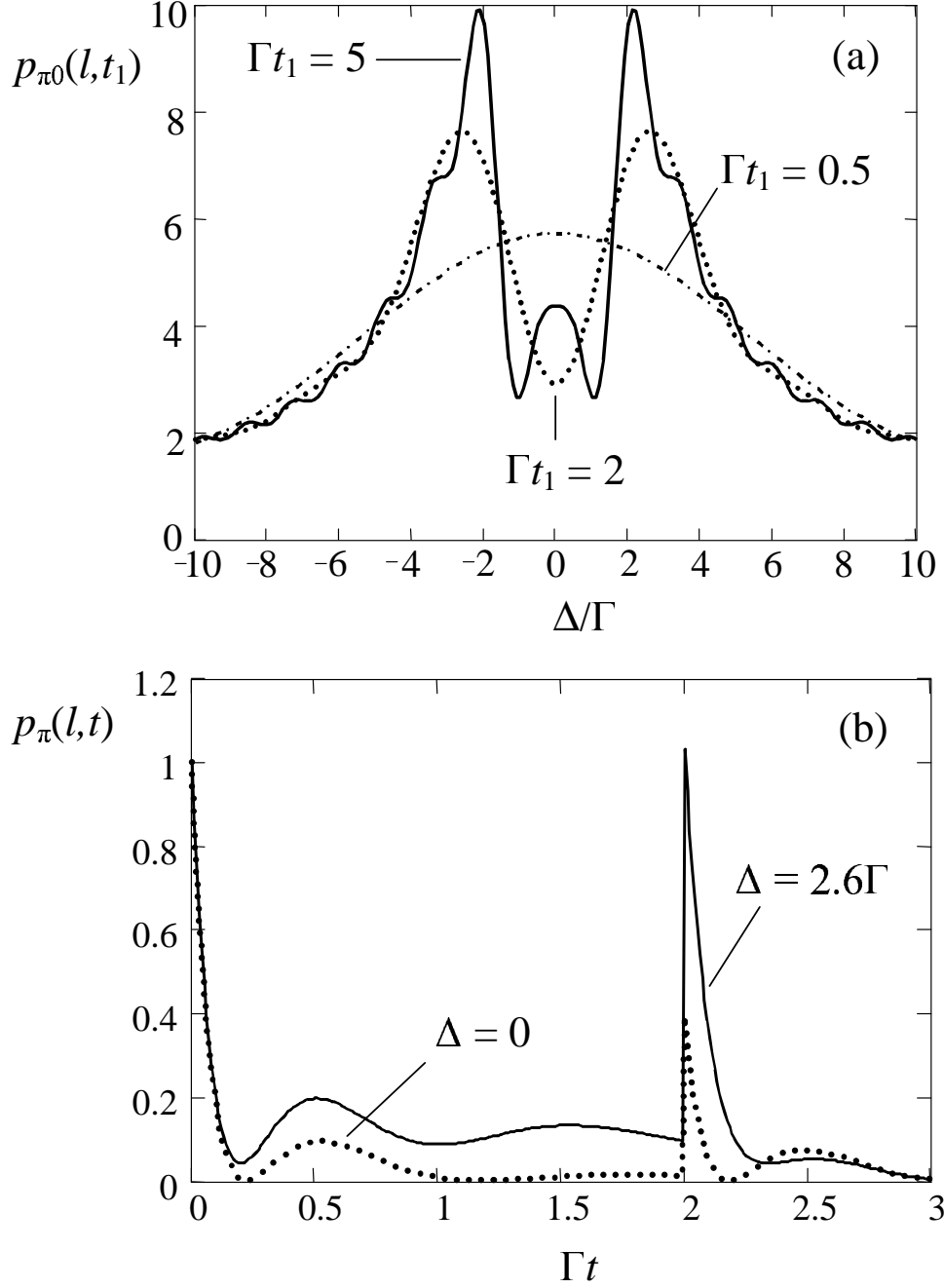


FIG. 2: (a) Resonant detuning dependence of the maximum probability of the radiation burst, $p_{\pi 0}(l, t_1)$ at time t_1 , when the phase of the input radiation changes to π . Plots are represented for the absorber with $T = 26$ and for different values of t_1 : $\Gamma t_1 = 5$ (solid line), $\Gamma t_1 = 2$ (dotted line), and $\Gamma t_1 = 0.5$ (dash-dotted line). (b) Time evolution of the detection probability $p_{\pi}(l, t)$ of the photon at the output of the absorber with optical thickness $T = 26$ if $\Gamma t_1 = 2$: solid line is for nonresonant case, $\Delta = 2.6\Gamma$, and dotted line is for resonant case, $\Delta = 0$.

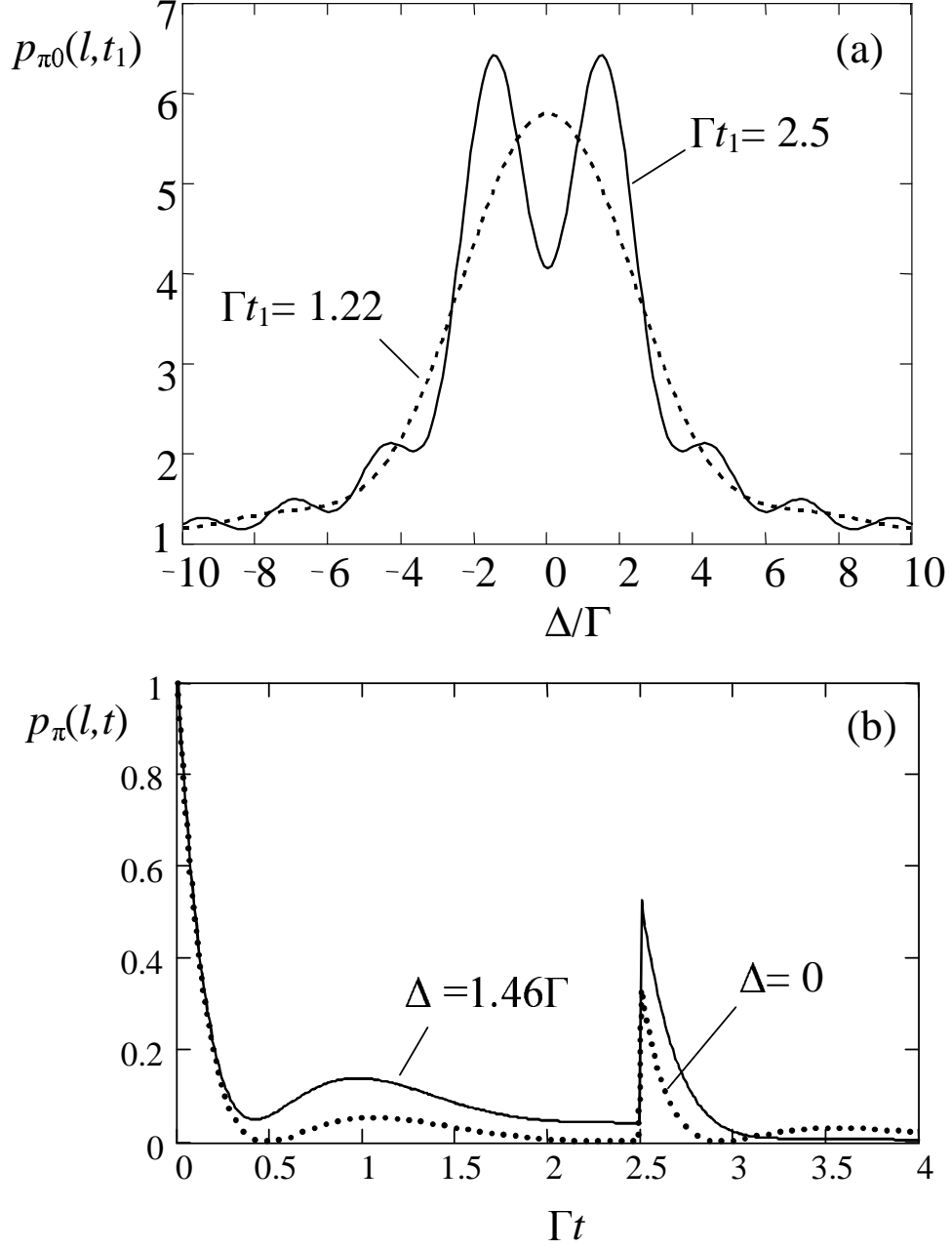


FIG. 3: (a) Dependence of the probability of the radiation burst, $p_{\pi 0}(l, t_1)$, on the resonant detuning Δ for $\Gamma t_1 = 2.5$ (solid line) and for $\Gamma t_1 = 1.22$ (dashed line). (b) Time dependence of the probability $p_{\pi}(l, t)$ for $\Delta = 1.46\Gamma$ (solid line) and for $\Delta = 0$ (dotted line). Optical thickness of the absorber is $T = 12$ for (a) and (b).

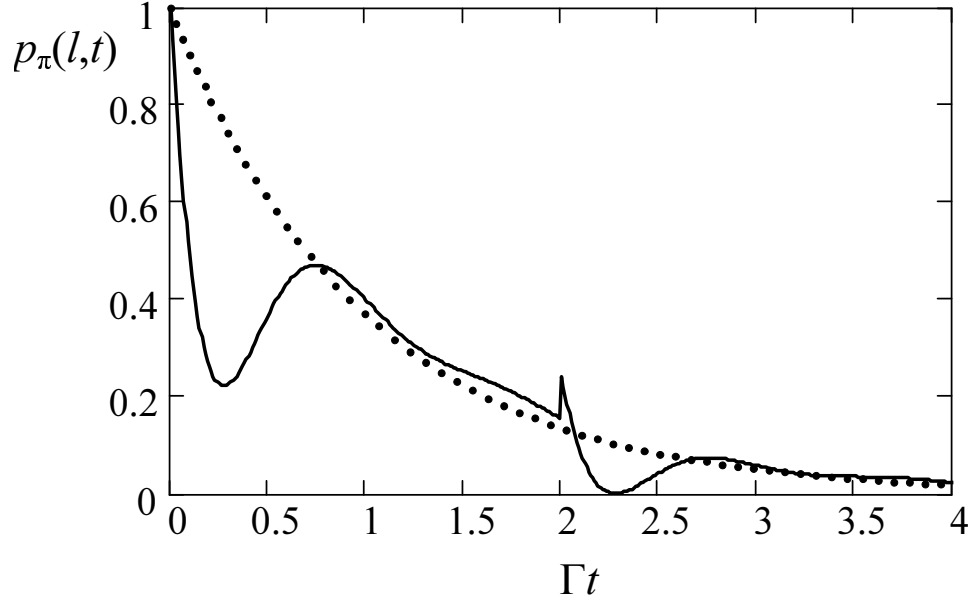


FIG. 4: Time evolution of the detection probability $p_\pi(l, t)$ of the radiation at the output of the absorber with optical thickness $T = 12$ (solid line). Input radiation changes its phase to π at time $t_1 = 2/\Gamma$. The resonant detuning is $\Delta = 4\Gamma$. Time evolution of the probability of the input radiation is shown by dots.

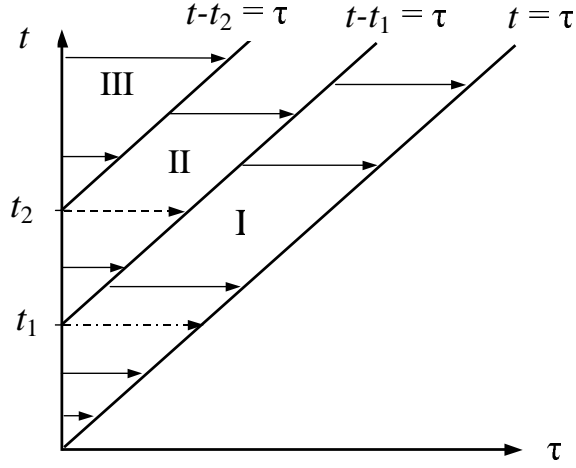


FIG. 5: Integration paths of the integral in Eq. (35). See the text for details

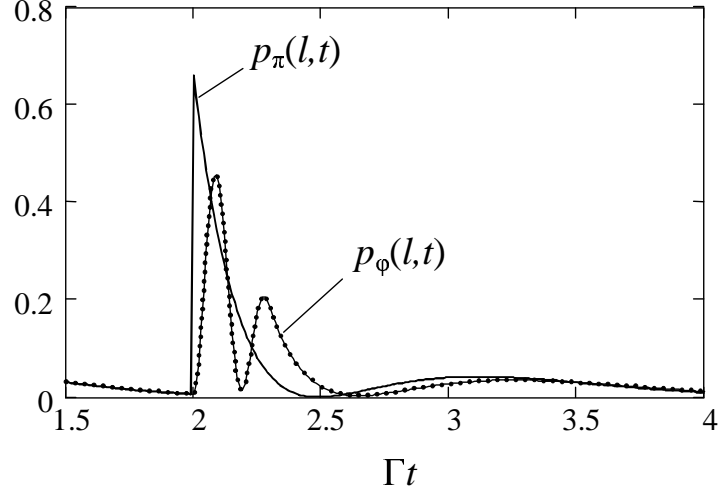


FIG. 6: Evolution of the output probability $p_{\pi}(l, t)$ after the phase shift of the input radiation field to π (bold solid line) and $p_{\phi}(l, t)$ during the frequency shift lasting between $t_1 = 2/\Gamma$ and $t_2 = 2.3/\Gamma$ (thin solid line). Dotted line shows the analytical approximation of the second case (see the text). The parameters are $b = 3\Gamma$ and $\delta\varphi = 10$ radian.

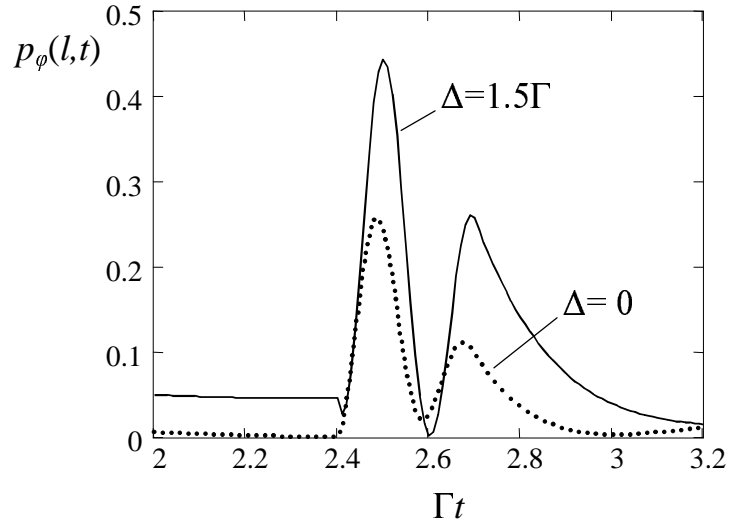


FIG. 7: Time evolution of the detection probability $p_{\phi}(l, t)$ of the photon at the output of the absorber with optical thickness $T = 12$ for resonant (dots) and nonresonant (solid line) excitations. The frequency shift of the radiation field $\delta\omega = 33.3\Gamma$ starts at time $t_1 = 2.4/\Gamma$ and terminates at $t_2 = 2.7/\Gamma$. The total phase shift of the radiation field is $\delta\varphi = 10$ radian.

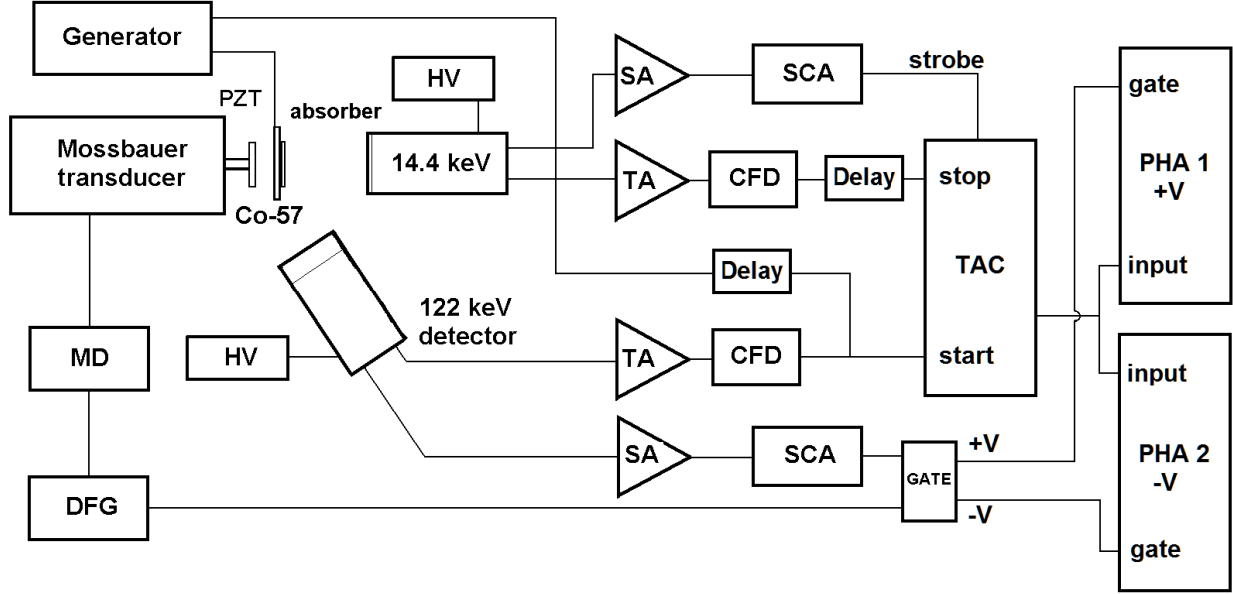


FIG. 8: Schematic layout of the experimental setup. TAC is a time to amplitude converter. PHA is a pulse-height analyzer. TA is a timing amplifier. SA is a spectroscopy amplifier. SCA is a single-channel analyzer. DFG-MD is the Mössbauer driving unit and function generator. HV is a high voltage supply. This setup differs from that, described in Ref. [30], by square-voltage-pulse Generator, synchronized via delay line with the pulse coming from the 122 keV detector. The square voltage pulse feeds PVDF transducer where the absorber is mounted.

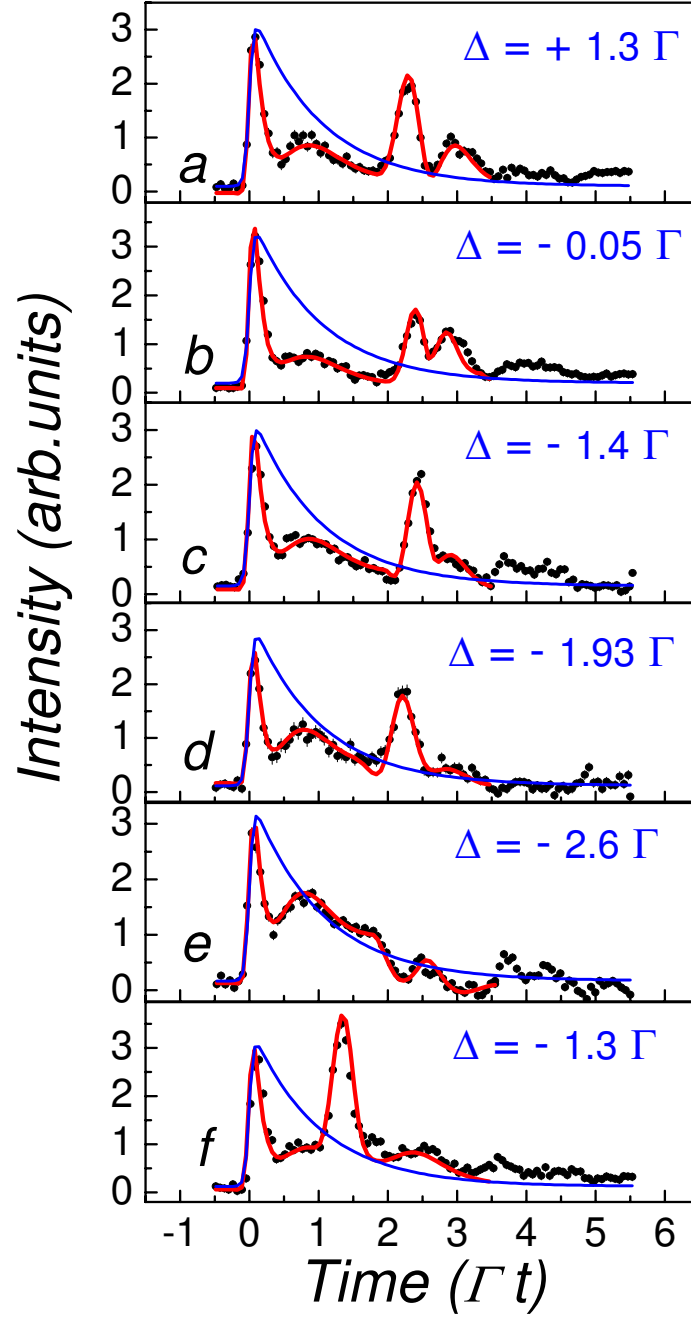


FIG. 9: (Color online) The delayed-coincidence spectra (dots) for the absorber with the effective thickness $T = 13.2$ and for different resonant detunings $\Delta = \omega_s - \omega_a$. Time t_1 , when a step voltage is applied to the PVDF transducer, is 280 nsec for a-e and 140 nsec for f. Voltage step is +10V except for e, where it is -4V. Thin solid line (in blue) shows the lifetime curve, measured without absorber. The thick solid line (in red) shows the theoretical fit.

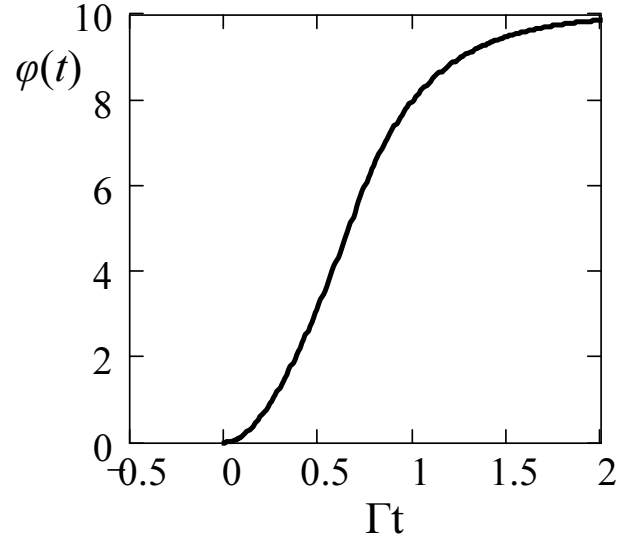


FIG. 10: Time dependence of phase $\varphi(t)$ obtained from the fitting of the theoretical model with experimental data. Maximum value of $\varphi(t)$ at $t \rightarrow \infty$ is taken 10 radian for visualization.

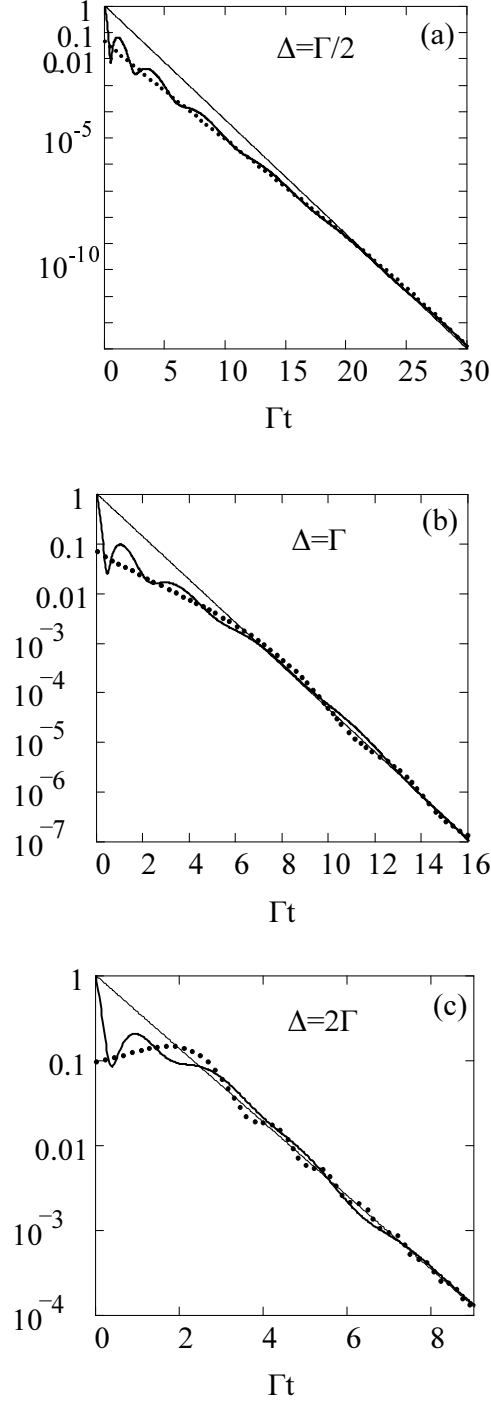


FIG. 11: Time dependence of the detection probability of the output photon, which is calculated with the help of exact value for the probability amplitude, given in Eq. (10) (thick solid line). Dotted line shows the result of the adiabatic approximation, given in Eq. (64). Thin solid line shows exponential decay of the probability of the input photon for comparison. The value of the resonant detuning Δ is given in each plot and $b = 3$. The vertical scale is logarithmic.

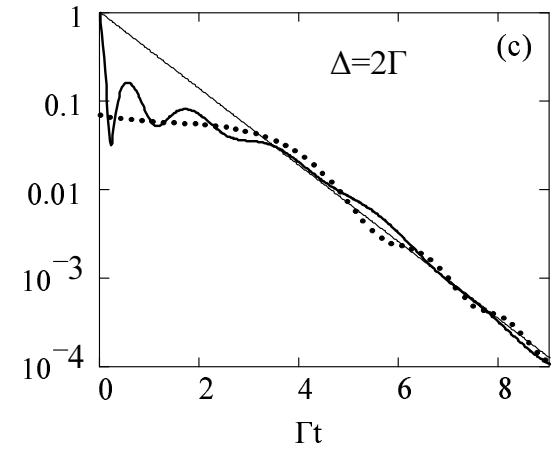
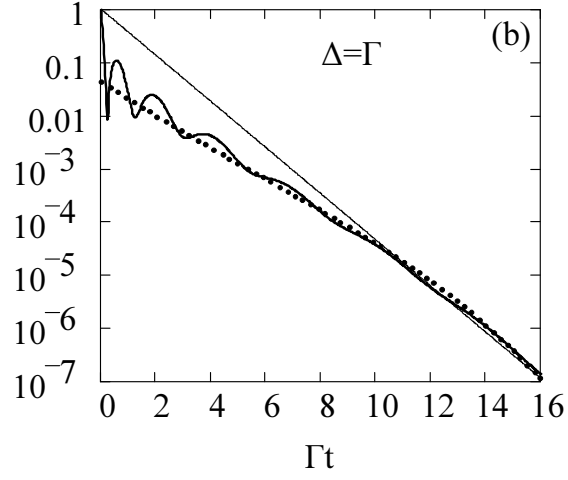
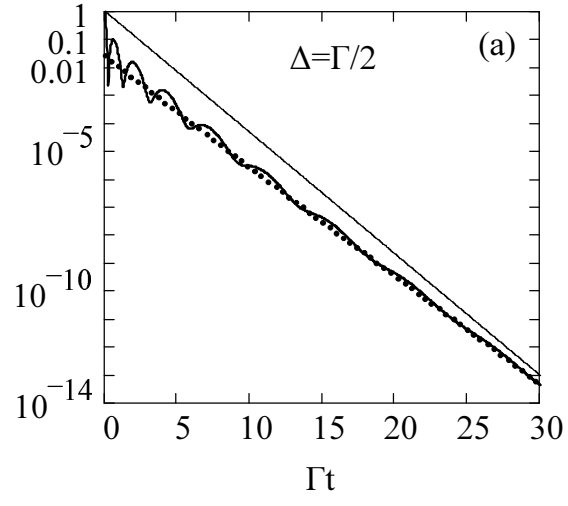


FIG. 12: The same plots as in Fig. 11 for $b = 6$.

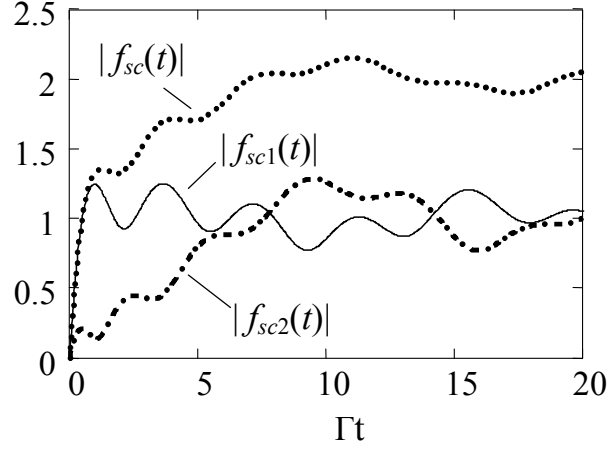


FIG. 13: Time dependence of the absolute value of the effective amplitude of the full scattered field $f_{sc}(t)$ (dotted line), of the fast component $f_{sc1}(t)$ (solid line) and of the slow component $f_{sc2}(t)$ (dash-dotted line). The parameters are $b = 3$ and $\Delta = 1$.

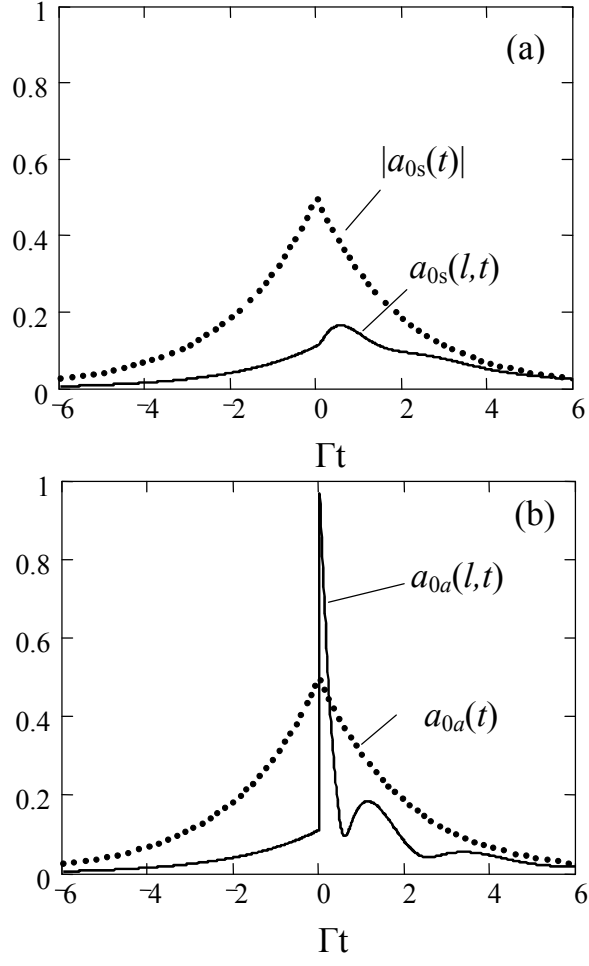


FIG. 14: Time dependence of the absolute values of the amplitudes of the symmetric (a) and asymmetric (b) components of the incident radiation field (dotted line). Their time dependence at the output of the resonant absorber is shown by solid lines. The parameters are $b = 3$ and $\Delta = 1$.

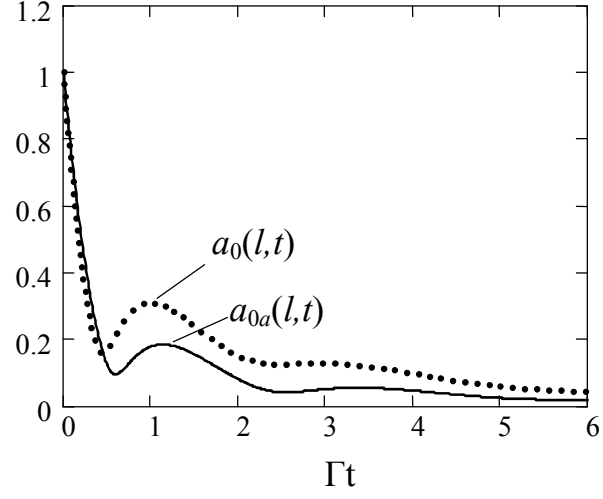


FIG. 15: Comparison of time dependence of the absolute value of the total amplitude of the output radiation field (dotted line) with that of the asymmetric part (solid line). The parameters are the same as in Fig. 14.